IN VITRO STUDIES OF THE DNA BINDING ACTIVITY OF THE OMPR PROTEIN

by

Adrienne Tardy

A THESIS

Presented to the Department of Biochemistry

and the Oregon Health Sciences University

School of Medicine

in partial fulfillment of the requirements for the degree of

Master of Science

March 1997

School of Medicine
Oregon Health Sciences University

This is to certify that the Master's Thesis of

Adrienne Tardy

has been approved

[redacted]
Dr. Linda J. Kenney

[redacted]
Dr. Hans Peter Bachinger

[redacted]
Dr. John Denu

[redacted]
Dr. Svetlana Lutsenko

[redacted]
Associate Dean for Graduate Studies

Table of Contents

List of Tables and Figures

Introduction

Materials and Methods

Acknowledgments

I am grateful to all members of the Kenney lab for their help in completing this work. Thanks especially to Linda Kenney for all of her guidance, support and patience -and for always making time for me.

Charlotte Head was an immense help in protein purification and C4 analysis as well as being wonderful to work with. Thanks to Hans-Peter Bachinger for advice and allowing me to work in his lab, and to Diane Mechling who solved countless CD spectra. I am grateful to Dick Brennan for helpful discussions. Thanks also to Svetlana Lutsenko and John Denu for all their advice.

Abstract

The prokaryotic transcription factor OmpR controls both the activation and repression of the outer membrane porin genes, *ompF* and *ompC*, in response to changes in osmolarity. Phosphorylation of the N-terminal domain of OmpR by the histidine kinase EnvZ leads to activation of its C-terminal domain by an unknown mechanism. OmpR binds tandem promoter regions in both *ompF* and *ompC* via a winged helix-turn-helix motif. The porin genes are regulated in a reciprocal manner which is poorly understood.

The purpose of this work is to biochemically characterize OmpR and to begin to test the current model of porin regulation. Toward this end, I have compared the DNA binding affinities of OmpR and OmpR-phosphate for different regions of its promoters. I have also compared the secondary structures of apo-OmpR and DNA-bound OmpR using circular dichroism. Results obtained thus far do not support the current genetic model of porin regulation in *Escherichia coli*.

Introduction

Bacterial adaptation and response to a wide range of external stimuli results from the coordinated regulation of various signal transduction pathways. Appropriate responses are essential for survival in different environments as well as the regulation of virulence in a number of important pathogens such as *Salmonella typhimurium, Vibrio cholerae* and *Bordatella pertussis.* One common mode of regulation is the two-component system which accounts for more than 60 types of signal response pathways throughout bacteria, yeast and plants. Cellular activities such as chemotaxis, nitrogen fixation and osmoregulation are all mediated by this type of system (Hoch, J. A. and T. J. Silhavy, 1995).

In its simplest form, a two-component regulatory system consists of two components, although many variations on this theme exist (Nixon *et al.*, 1986). The first component is a sensor which is a histidine kinase that is autophosphorylated in the presence of ATP (Hess, J. F. *et al.*, 1988). The second is a response regulator which is phosphorylated by the sensor on a specific aspartic acid residue in a Mg^{2+}-dependent manner (Stock, J. B. *et al.*, 1989). These effectors typically reside in the cytoplasm and often regulate transcription (Stock, J. B. *et al.*, 1989). Most response regulators consist of an N-terminal receiver domain usually coupled via a linker region to a C-terminal output domain. Although response regulators differ widely in their primary sequences, it is presumed that they share structural similarity in

their N-terminal regulatory domains (Volz, K., 1993). One member of this superfamily is the outer membrane porin regulator OmpR, the two domain response regulator of *E. coli* K12, *Salmonella typhimurium* and *Salmonella typhi* porin gene expression. OmpR belongs to a subfamily including more than 40 proteins with homologous C-terminal binding domains of approximately 100 amino acid residues (Martinez-Hackert, E. and A. M. Stock, 1997).

OmpR acts together with the histidine kinase EnvZ to regulate expression of the porin genes, *ompF* and *ompC*, in response to changes in osmolarity (van Alphen, W. *et al.*, 1977). The proteins OmpF and OmpC are trimeric outer membrane pores that allow passive diffusion of small hydrophilic molecules across a hydrophobic barrier (Nikaido, H. and M. Vaara, 1985). The exclusion limit of both pores is about 600 Da, but the rates of diffusion through the porins differ considerably (Nikaido, H. and M. Vaara., 1985; Payne, J. W., 1968). The total amount of porins in a cell is constant, but their relative levels fluctuate with respect to osmolarity, temperature, pH and carbon source (Datta D. B. *et al.*, 1976). The OmpF pore has a diameter of 1.16 nm and is the larger of the two porins. It is produced in higher amounts at low osmolarity (Nikaido, H. *et al.*, 1987). OmpC has a smaller pore with a diameter of 1.08 nm and as a result, has a slower flow rate (Figure 1). It is the predominant porin present at high osmolarity.

Regulation of the porins requires the inner membrane protein kinase,

EnvZ (Liljestrom, P., 1986). EnvZ is 450 amino acids in length and has two transmembrane domains (Forst, S. J. *et al.*, 1987). The N-terminal portion is located in the periplasm and presumably senses the osmolarity of its surroundings (Hoch, J. A. and T. J. Silhavy, 1995). The signal that EnvZ senses is entirely unknown, but the periplasmic domain is required (Tokishita, S. A. *et al.*, 1991; Igo, M. and T. J. Silhavy, 1988). A signal controlling the rate of autophosphorylation of EnvZ at H243 is transduced across the inner membrane to the C-terminus (Roberts, D. L. *et al.*, 1994). Phosphotransfer is a bimolecular reaction in which the kinase domain of one monomer binds ATP and catalyzes the phosphorylation of a histidine residue on an adjactent monomer (Yang. Y., and M. Inouye, 1991). The C-terminus of EnvZ in turn communicates with the N-terminus of OmpR and, depending on its phosphorylation state, behaves as either an OmpR phosphatase or kinase (Igo, M. *et al.*, 1989b).

OmpR is a cytoplasmic protein that consists of 239 amino acids and acts as a transcriptional regulator of the porin genes (Wurtzel, E. T. *et al.*, 1982). Phosphorylation by EnvZ at D55 stimulates binding to promoter regions at both *ompF* and *ompC* (Delgado, J. and M. Inouye, 1993; Forst, S. *et al.*, 1989). Gel shift assays and DNase I footprinting have compared the DNA binding ability of OmpR and OmpR-P *in vitro* (Aiba, H. *et al.*, 1989). An enhancement in affinity is observed with OmpR-P. Another group observes a two-fold increase in affinity of OmpR-P compared to OmpR (Huang, K. and M. Igo,

1996). However, the degree to which phosphorylation stimulates DNA binding is unknown, because the proportion of OmpR-P in the assays has not been quantified.

The *ompR* and *envZ* genes are transcribed as an operon from the *ompB* locus (Wurtzel, E.T. *et al.*, 1982; Mizuno, T. *et al.*, 1982). *envZ* is downstream from *ompR*, and organized such that the termination sequence of *ompR* overlaps the initiation sequence of *envZ*. Nonsense mutations in *ompR* have polar effects on *envZ*, demonstrating that translation of *envZ* requires complete translation of *ompR*. Translation of the two genes was monitored by creating protein fusions of *lacZ* to *ompR* and *envZ*. Results indicated that translation of *ompR* was approximately 8 times more efficient than translation of *envZ* (Liljestrom, P., 1986), producing OmpR protein in great excess compared to EnvZ.

The current model, based largely on genetic analysis, is as follows: at low osmolarity EnvZ autokinase activity is low, resulting in low levels of OmpR-P (Russo, F. and T. J. Silhavy, 1991; Pratt L. A. and T. J. Silhavy, 1995). OmpR-P binds to high affinity sites at *ompF*, activating its transcription. At higher osmolarity, EnvZ autokinase activity increases, leading to higher levels of OmpR-P. OmpR-P binds to lower affinity sites at *ompF*, presumably by forming a repressive loop that inhibits *ompF* transcription (Huang, K. *et al.*, 1994). OmpR-P also binds to lower affinity sites at *ompC*, resulting in transcriptional activation of this gene. In strains lacking *envZ*, there is very

little porin production, indicating that unphosphorylated OmpR has little, if any activity (Mizuno, T. and S. Mizushima, 1987). Therefore, by varying the concentration of a single species, OmpR-P, it is proposed that the reciprocal regulation of the porin genes is achieved (Figure 2; Russo, F. and T. J. Silhavy, 1991).

The *ompF* promoter is composed of four OmpR binding sites (F1-F4) based on footprinting data (Huang, K. and M. Igo, 1996). A single OmpR binding site contains 18 basepairs and is comprised of two half sites (Figure 3). It is characterized by a highly conserved central GxxxC sequence, where the G and C are separated by 3 nucleotides (Huang, K. and M. Igo, 1996). F1, F2 and F3 are arranged in tandem (Maeda, S. *et al.*, 1991; Huang, K. and M. Igo, 1996), but according to gel migration analysis, only F1 is capable of binding OmpR independently. Binding at F2 and F3 may therefore depend on cooperative interactions with OmpR bound to F1 (Huang, K. and M. Igo, 1996). F1 has two repeating AC nucleotides at positions 1, 2 and 11, 12 that are separated by approximately 10 basepairs. F2 only has an AC pair at positions 11, 12 and F3 lacks an AC pair at the appropriate positions altogether. Huang *et al.* inactivated half of the F1 site by random mutagenesis and used gel shift assays to demonstrate that OmpR is unable to bind these F1 mutants. This implies that two adjacent half sites are required for OmpR binding, and that cooperative interactions between OmpR molecules may be required for stable complex formation.

F4, which is located about 250 base pairs upstream of F1, has been identified as a distal OmpR binding site (Huang, K. *et al.*, 1994). Insertion of a 22 bp fragment between the F1 and F4 sites abolishes repression of *ompF* expression. Thus, F4 is thought to be involved in negative regulation of *ompF*. At the -70 and -110 position of *ompF*, there is an intrinsic bend in the DNA (Mizuno, T., 1987). In addition, integration host factor (IHF) binds at sites located at both -60 and -170 (Ramani, N. *et al.*, 1992). IHF is a protein that bends DNA into a conformation that is favorable for protein-protein interactions. Strains that are deleted for IHF are constitutive for *ompF* expression (Tsui *et al.*, 1988). Based on the above observations, negative regulation of the *ompF* promoter is most likely achieved via repressive loop formation.

Efficient transcriptional initiation at the *ompF* promoter involves several factors in addition to OmpR. There is evidence that integration host factor, IHF (Ramani, N. *et al.*, 1992; Tsui, P. *et al.*, 1988), leucine repressor protein, Lrp, (Ernsting, B. *et al.*, 1992) catabolite activator protein, CAP, (Scott, N. and C. Harwood, 1980) and nucleoid associated DNA binding protein, H-NS (Graeme, C. *et al.*, 1989) interact with *ompF*. In addition, genetic studies indicate that suppressors of mutations in *ompR* which restore activity map to the α-subunit, suggesting that an interaction between OmpR and the α–subunit of RNAP occurs (Slauch, J. M. and T. J. Silhavy, 1991; Sharif, T. R. and M. Igo, 1993). The suppressors map to the C-terminal domain of *rpoA*

and deletions in this region result in the repression of transcription from *ompF* and *ompC* (Russo, F. *et al.*, 1993; Pratt, L. A. *et al.*, 1994).

At the *ompC* promoter there are three tandem binding sites for OmpR, C1, C2 and C3 (Maeda, S. and T. Mizuno, 1990). C1 is the only site of the three with AC nucleotides at positions 1, 2 and 11, 12 in both half sites and is reportedly the only *ompC* site capable of independent OmpR binding (Igo, M., unpublished results). The working model predicts that these are low affinity sites for OmpR-P that lead to activation of *ompC* at high osmolarity.

OmpR is homologous to other response regulators in its N-terminal domain. The structures of both CheY and NarL, proteins in different subfamilies, have been solved crystallographically (Stock, J. B. *et al.*, 1989; Volz, K. and P. Matsumura, 1991; Baikolov, I. *et al.*, 1996). Using information from their solved structures as well as sequence alignments, it is proposed that OmpR consists of two domains that are attached by a flexible linker. The N-terminal domain is a doubly wound α/β domain with five α-helices surrounding a five stranded parallel β-Sheet (Figure 4). An acidic pocket contains the aspartic acid residue which undergoes phosphorylation, D55 (Delgado, J. and M. Inouye, 1993), as well as the highly conserved residues D12, D13, T83, and K105. A Mg^{2+} ion sits in this pocket, and is thought to facilitate the formation of an acyl phosphate, stabilizing the negative charge of the active site (Lukat, G. S. *et al.*, 1990).

Recently the crystal structure of the C-terminal domain of OmpR was

solved (Martinez-Hackert, E. and A. M. Stock, 1997). It contains a winged-helix-turn-helix (HTH) DNA binding motif comprised of three α–helices packed against two antiparallel β–sheets (Figure 5). This motif was not recognized by examination of the primary sequence, because there was a lack of primary sequence homology between the DNA binding domain of OmpR and other DNA binding proteins whose structures were known. This is partly due to two notable features in OmpR. One structural difference between OmpRc and other winged HTH proteins is the presence of a four stranded antiparallel β–sheet preceding the DNA binding domain. The β–sheet resides between the N-terminal regulatory domain and the HTH motif. It packs against helices α1 and α3, thereby contributing to the hydrophobic core of OmpRc (Martinez-Hackert, E. and A. M. Stock, 1997). Second, loops connecting helix α2 to helix α3 and helix α3 with the C-terminal hairpin are significantly longer, at 10 and 8 amino acid residues respectively, than those typically found in other proteins (Suzuki, M. and S. E. Brenner, 1995). Mutations in OmpR that lack the ability to interact with the α–subunit of RNAP (RpoA; Slauch, J. M. *et al.*, 1991) localize primarily to the 10-residue α–loop connecting helix α2 to α3. These mutations all lie on one surface of the protein in the crystal structure and are thus likely to be part of an interaction surface between OmpR and RNAP (Martinez-Hackert, E. and

A. M. Stock, 1997).

By analogy to members of the winged HTH family of proteins, helix α3 is the DNA recognition helix and the loop connecting β–strands β6 and β7 functions as the DNA recognition wing. However, in the crystal structure it is not possible to position amino acids that lie at both ends of the recognition helix near the DNA (Martinez-Hackert, E. and A. M. Stock, 1997). Mutagenesis data indicate that both ends of the helix are important for DNA binding (Russo, F. *et al.*, 1993; Aiba, H. *et al.*, 1994). This suggests that OmpR may undergo a confomational change in order to bind DNA. Alternatively, it may be the DNA which changes conformation upon complex formation or both the OmpR and the DNA that change conformation upon binding.

One important question about the OmpR protein which presently remains unanswered is whether OmpR exists as a dimer or monomer in solution. The unphosphorylated form reportedly exists as a monomer in solution (Harlocker, S. *et al.*, 1995; Jo, Y. *et al.*, 1986), but is unable to form stable protein-DNA complexes as a monomer (Huang, K. and M. Igo, 1996). Activation of OmpR by phosphorylation at D55 has been proposed to shift the equilibrium from monomer to dimer. Higher molecular weight complexes of OmpR have only been detected when the protein was phosphorylated in the presence of cross-linking agents (Nakashima, K. *et al.*, 1991). The closely related PhoB protein elutes from an HPLC column as two peaks when phosphorylated. One of the peaks elutes at a similar position to that of a

chemically cross-linked dimer of PhoB (McCleary, W., 1996). Because little is known about OmpR dimerization, the regions that are important for this interaction have not been defined. However, the mutations G96A and R115S (located in the N-terminal domain just before the linker region), have been isolated as mutants that prevent oligomerization and DNA binding in response to phosphorylation (Nakashima K. *et al.*, 1991). Other groups have suggested that the C-terminal domain is important for dimerization (Tsuzuki, M. *et al.*, 1994; Harlocker, S., 1996). An OmpRc mutant, G227C, was isolated which formed a stable dimer in the absence of the N-terminal domain. It was proposed that the activator domain of OmpR may be located in the C-terminal domain (Tsuzuki, M. *et al.*, 1994).

Although EnvZ is the primary phosphodonor for OmpR *in vivo*, it can be phosphorylated when incubated with ^{32}P-labeled acetyl phophate (Kenney, L. J. *et al.*, 1995). Studies with response regulators using small chemical phosphorylating agents have demonstrated that these molecules are capable of acting as effectors of gene expression (Wanner, B. L. and M. R. Wilmes-Riesenberg, 1992). Amino acid analysis of OmpR phosphorylated in the presence of acetyl phosphate has revealed that only one aspartic acid residue is phosphorylated and that it is D55 (Head, C. and L. J. Kenney, unpublished data). PhoB, a protein in the same subfamily as OmpR has been shown to have a K_m of 7-8 mM for acetyl phosphate (McCleary, W., 1996). Since intracellular concentrations of acetyl phosphate can exceed 1 mM, the K_m

value is consistent with a possible *in vivo* role for this compound (McCleary, W., 1993). This type of activation demonstrates that response regulators catalyze their own phosphorylation in the presence of an appropriate phosphodonor (Lukat, G. *et al.*, 1992).

An issue which remains unresolved is the mechanism by which phosphorylation of OmpR activates transcription (Martinez-Hackert, E. and A. M. Stock, 1997). One possibility is that protein dimerization or a change in conformation occurs that places the C-terminal domain in a more favorable orientation in order to effect its function. In the crystal structure of NarL, the N-terminal domain packs directly against one face of the recognition helix, thereby preventing access to its HTH region which would prevent DNA binding (Baikolov, I. *et al.*, 1996). Activation of NarL via phosphorylation presumably disrupts the interaction between the N- and C-terminal domain. If the HTH motif in OmpR is aligned with that of NarL, the N-terminal domain of NarL collides with the C-terminal β–hairpin of OmpRc (Martinez-Hackert, E. and A. M. Stock, 1997). Thus, it is evident that the N-terminal domains in these two subfamilies of response regulators are positioned differently with respect to their recognition helices. A crystal structure of intact OmpR may reveal how its two domains are situated with respect to each other.

Osmoregulation in *E. coli*

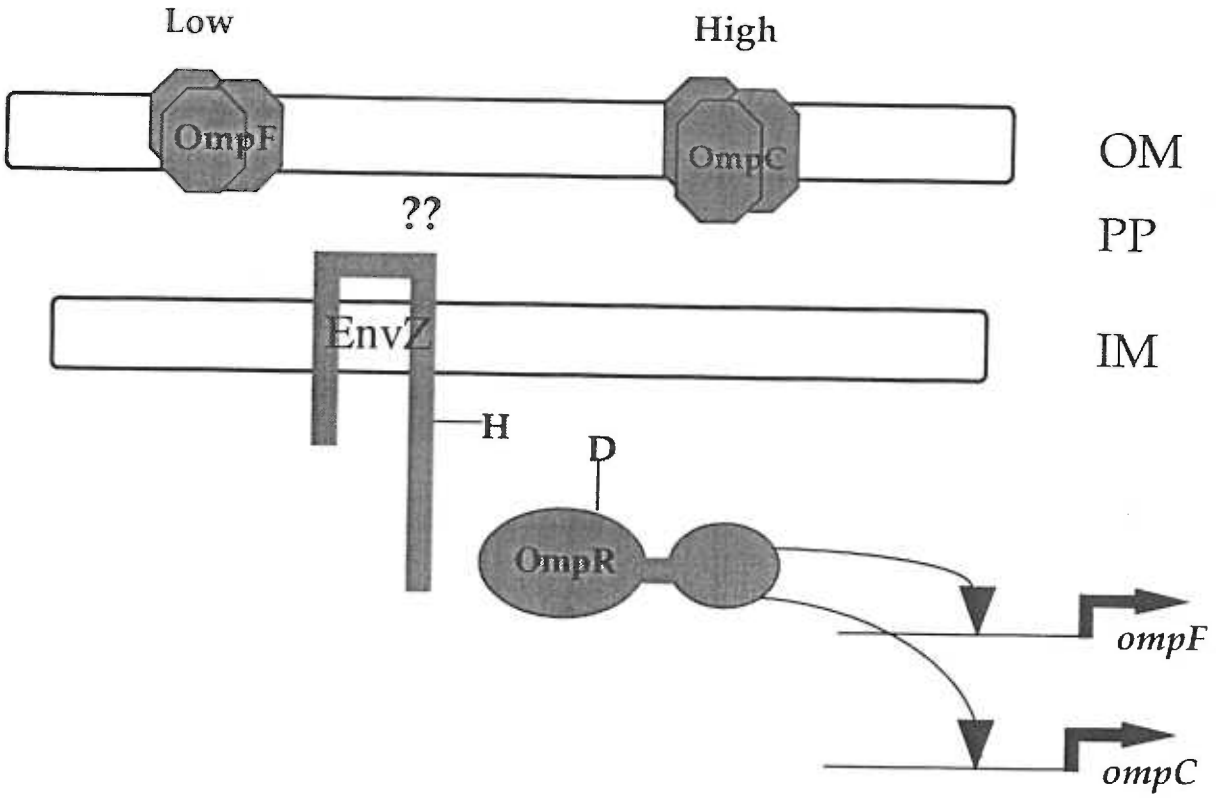

Figure 1. Overview of the porin regulation system in *Escherichia coli*. OmpF and OmpC are trimeric proteins that function as porins in the outer membrane. Regulation of their genes *ompF* and *ompC* is accomplished by a two-component regulatory system. EnvZ serves as the sensor kinase that phosphorylates the response regulator OmpR, which controls expression of *ompF* and *ompC*.

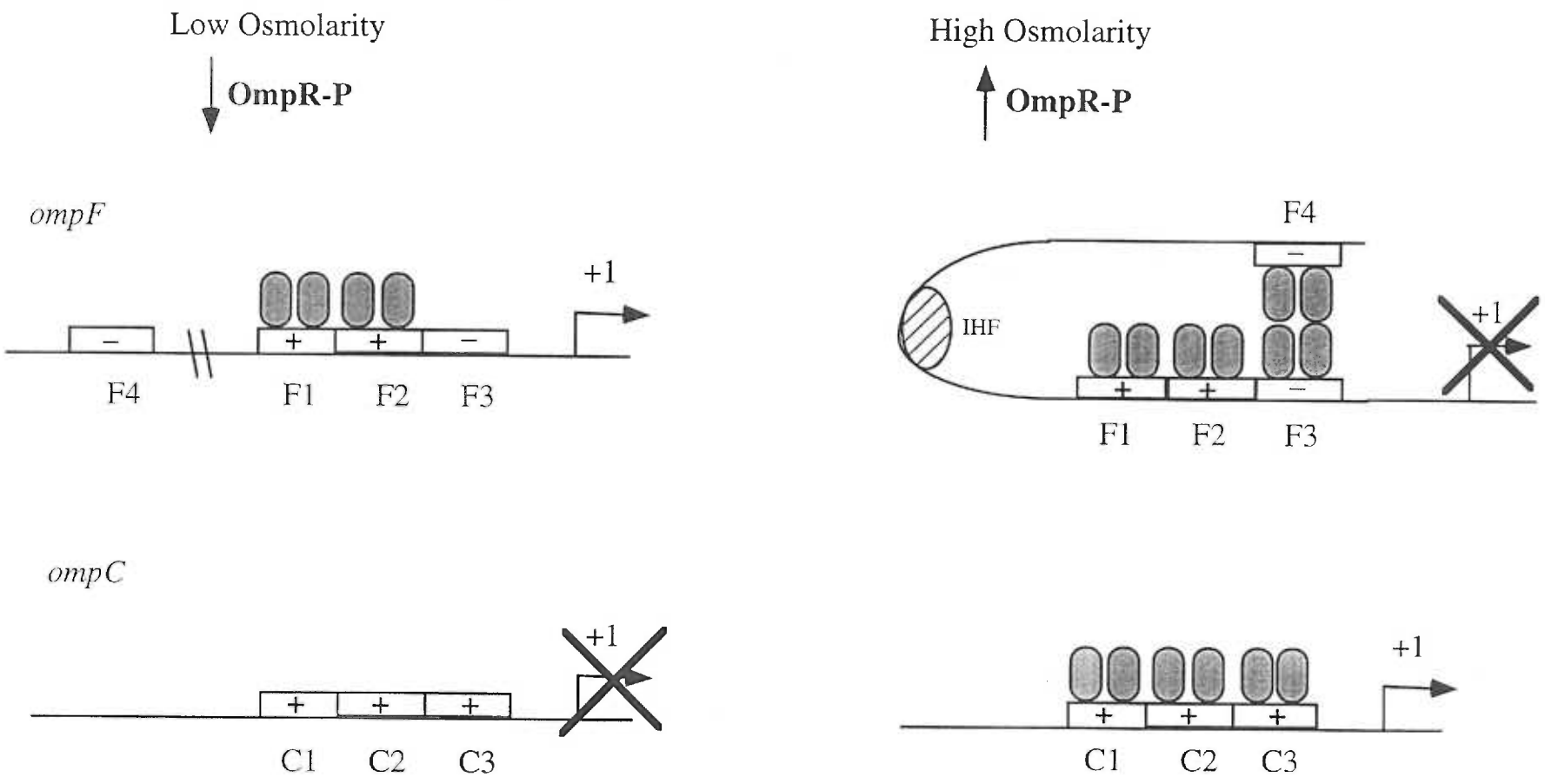

Figure 2. Current model of *ompF* and *ompC* regulation by OmpR. At low osmolarity OmpR-P is bound to high affinity sites, resulting in transcriptional activation. At higher osmolarity, OmpR-P binds to lower affinity sites at both *ompF* and *ompC*, leading to repression of *ompF* and activation of *ompC*. Repression at *ompF* is thought to involve a loop formation of the DNA in which IHF bends the DNA between F1 and F4. Filled ovals represent OmpR monomers.

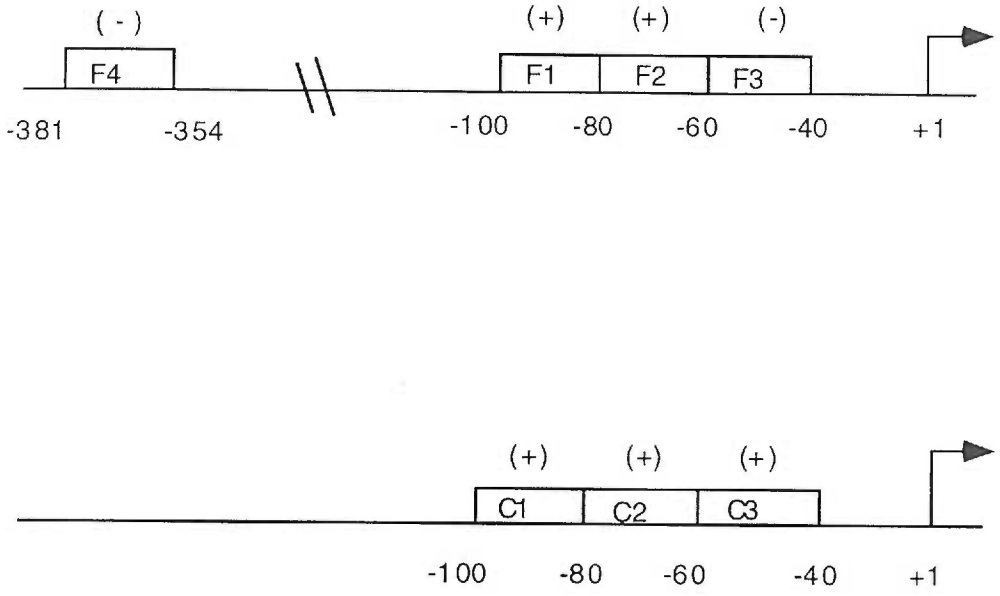

F1 ACTTTTGGTTACATATTT

F2 TCTTTTTGAAACCAAATC

F3 TATCTTTGTAGCACTTTC

C1 ACATTTTGAAACATCTAT

C2 GATAAATGAAACATCTTA

C3 AGTTTTAGTATCATATTC

Figure 3. Porin promoters. The regions thought to be required for positive (+) and negative (-) regulation. Sequences of binding sites are depicted below. The characteristic feature is a G and C pair separated by 3 nucleotides.

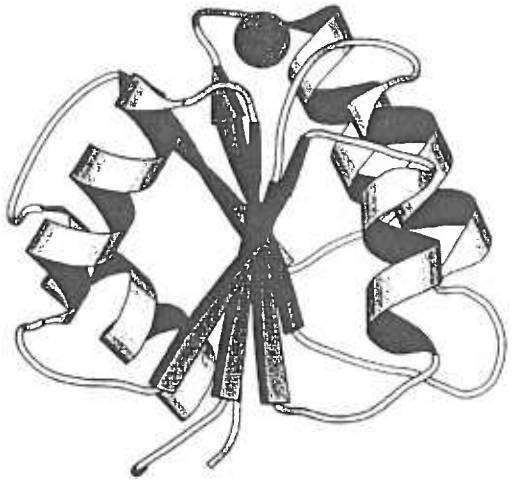

Figure 4. Ribbon drawing of the chemotaxis response regulator, CheY with a bound Mg^{2+} at the active site (Stock, A., *et. al.*, 1993). The core consists of 5 parallel β–sheets surrounded by 5 α–helices.

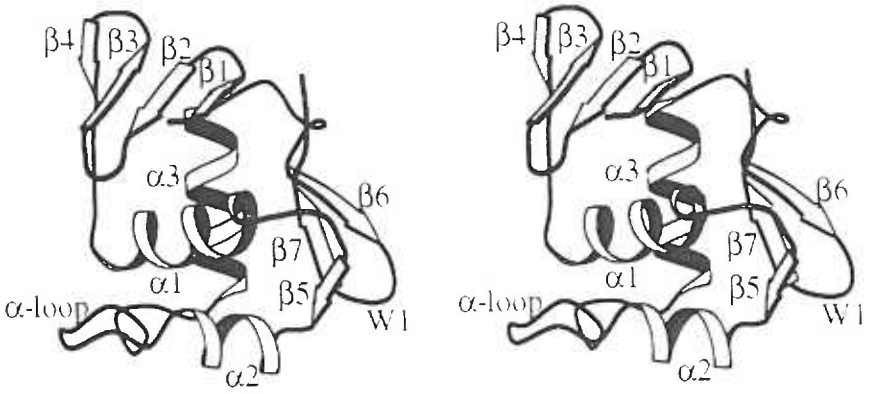

Figure 5. Ribbon drawing of the C-terminal domain of OmpR (Martinez-Hackert, E., *et. al* 1997). Helices α2 and 3 comprise the helix-turn-helix DNA binding motif. The α-loop is surface exposed and has been proposed as a possible site of interaction with the α-subunit of RNA polymerase.

Materials and Methods

Abbreviations

OmpR- outer membrane porin regulator
OmpR-P- OmpR phosphate
EnvZ- envelope protein
RNAP- RNA polymerase
OmpRc- C-terminal domain of OmpR
OmpRn- N-terminal domain of OmpR
RpoA- α-subunit of RNA polymerase
α-CTD- C-terminal domain of RpoA
EDTA- ethylenediamine tetraacteic acid
DTT- 1,4-dithiothreitol
IPTG- isopropyl β-D-thiogalactopyranoside
LB- Luria broth
RT- room temperature
PAGE- polyacrylamide gel electrophoresis
SDS- sodium dodecyl sulfate
kDa- kilodalton
AEBSF- 4-(2-Aminoethyl)-Benzenesulfonyl fluoride hydrochloride
CD- circular dichroism
K_d- dissociation constant
FA- fluorescence anisotropy

Protein purification. OmpR was overproduced from the plasmid pFR28 (Fig. 1, Russo, F. and T. J. Silhavy, 1991), which encodes *ompR* under control of the *lac* promoter. pFR28 was expressed in an *E. Coli* K-12 derivative CH1 (MC4100 Δ*envZ*-AT142, Sarma, V. and P. Reeves, 1977) containing the *envZ* deletion from strain AT142 (Mizuno, T. and S. Mizushima, 1987b). Cells were grown in LB containing 100 μg/ml ampicillin at 37°C and induced with 1 mM IPTG at mid-logarithmic phase of growth. After 16 hours, the cells were harvested by centrifugation and resuspended in TGED [20mM Tris-HCl, pH 7.6, 5% glycerol (v/v), 0.1 mM EDTA, 0.1 mM

DTT], 50 mM NaCl and 1 mM AEBSF. Bacteria were lysed by two passages through a French pressure cell at 900 p.s.i. The bacterial extracts were centrifuged at 32,000 rpm (100,000xg in a Beckman L8-80M ultracentrifuge) for 90 minutes to remove unlysed cells and membranes. The supernatant was precipitated with $(NH_4)_2SO_4$ (45% saturation at 0°C) and centrifuged at 10,000 rpm (J2-21 Beckman). The pellet was resuspended in TGED, dialyzed overnight against TGED (4°C) and applied to a DEAE Sephacell anion exchange column. The gradient ranged from 0-500 mM NaCl, the flow rate was 0.75 ml/min, and the elution volume was 500 ml. OmpR eluted around 200 mM NaCl. OmpR fractions were pooled, dialyzed against TGED + 70 mM NaCl and concentrated in an Amicon ultrafiltration cone (25 kDa membrane cut-off) to a volume of 50 ml. The sample was then applied to a SP-Sepharose cation exchange column and eluted with a NaCl gradient ranging from 0-500 mM. OmpR eluted at approximately 300 mM NaCl. Fractions containing OmpR were analyzed by 12% SDS-PAGE and fractions greater than 95% pure were combined.

Purification of mutant OmpR. *ompR* was subcloned from pFR28 into pET-11a (Fig. 1, Novagen) using the *NdeI* and *BamHI* restriction sites. Plasmid pET-11a containing *ompR* under the control of the T7 promoter of RNA polymerase was transformed into the *E. Coli* strain BL21(DE3) (Novagen). Growth of cells and protein purification was carried out as described for OmpR except that after induction by 0.25M IPTG, cells were

cultured at 25°C for 5 hours and then harvested.

Mutagenesis. OmpR was subcloned into p-SELECT (Promega) from pET-11a using the *Xba1* and *HindIII* restriction sites. Oligonucleotides containing the desired mutations and analytic restriction sites were synthesized. Sequences were **5′ ATG GCT TGT CGA TAT CCC GAC GTC TTC G 3′** for OmpR-C67S containing an *EcoRV* restriction site, **5′ CGA CTA CAT TCC GAG ACC GTT TAA CCC G 3′** for OmpR-K105R including a *BsaI* restriction site, **5′ TCT TAT GGT ACT CGA GTT AAT GTT ACC TG 3′** for OmpR D55E with a *XhoI* restriction site. Double stranded p-SELECT-*ompR* was denatured and allowed to anneal in the presence of the mutagenic oligonucleotide and an ampicillin repair primer. After synthesis of a complementary strand, the product was transformed into a *recA*$^-$ strain, ES1301mutS (Promega), using ampicillin selection. Plasmid DNA was then isolated and transformed into strain JM109 and ampicillin resistant colonies were isolated. Mini plasmid DNA was isolated and products which contained the restriction site in the mutagenic oligonucleotide were subcloned into the pET-11a expression vector. OmpR-C67S was confirmed by dideoxy DNA sequencing using the T7 promoter site as a primer (kindly sequenced by Tom Keller, OHSU). OmpR-K105R was confirmed by mass spectral analysis (Dr. Joe Loo, Parke-Davis).

Phosphorylation of OmpR. 20 μM OmpR was incubated for 40 minutes in the presence of 20 mM acetyl phosphate (Sigma), 20 mM $MgCl_2$, 50 mM

NaCl and 5mM Na_2HPO_4/NaH_2PO_4 pH 7.4 at RT. The percentage of phosphorylated OmpR in the sample was determined by separating OmpR from OmpR-P on a C4 reverse phase HPLC column (Figure 2, IBM LC/9533 System). OmpR and OmpR-P were eluted as two distinct peaks, the earlier of which was OmpR-P. Areas under the peaks were integrated in order to determine the proportion of OmpR-P (C4 analysis performed by Charlotte Head).

Trypsin Proteolysis. 400 pmol of OmpR or OmpR-P (approximately 30% phosphorylated after incubation with acetyl phosphate), in the presence or absence of an equimolar concentration of F1 DNA, was incubated in a buffer containing 140 mM Imidazole pH 7.6, 1 mM EDTA, and trypsin (protein to trypsin ratio of 100:1 (w/w)). After 12 minutes at 37°C the reaction was stopped by the addition of a five fold excess of AEBSF protease inhibitor and the samples were quick-frozen in a dry ice methanol bath. Sample buffer (4x) was added (0.25 M Tris-HCl, pH 6.8, 40% glycerol, 8% SDS, 0.4% bromophenol blue) and the samples were incubated at 65°C for 5 minutes. Protein fragments were resolved by PAGE on a 16% Tris-tricine, 8M urea polyacrylamide gel (Schagger, H. and G. vonJagow, 1987).

Dynamic Light Scattering. A DynaPro-801 Molecular Sizing Instrument was used to perform dynamic light scattering experiments. 5 mg/ml of OmpR and OmpR-P (~30% OmpR-P) protein was suspended in a buffer containing (mM) 20 TrisHCl pH 7.6, 20 $(NH_4)_2SO_4$, 250 NaCl and 2 DTT

and filtered through a 0.1 μm pore membrane (Whatman, Anatop 10). The samples were injected into the instrument and measurements of the average radius were taken every 20 seconds for approximately 5 minutes. Measurements with a sum of squares error of less than 5.0 were used in calculating the average estimated molecular weight.

Gel Filtration. OmpR, OmpR-P and OmpR-K105R were loaded onto a Superdex-75 gel filtration column at a concentration of 0.7 mg/ml in 50 mM NaCl, 5mM Na_2HPO_4/NaH_2PO_4 pH 7.4 and 0.05% Tween 20 and eluted in the same buffer. The elution profile of OmpR was compared to BSA (67 kDa), ovalbumin (25 kDa) and chymotrypsinogen (44 kDa) protein standards at 1 mg/ml.

Porin phenotype of the mutants. Outer membrane fractions were isolated in order to examine the porin expression pattern in the presence of the various mutant OmpR proteins described here. The outer membrane fractions were prepared as follows: The *ompR* deletion strain (MH1160) was transformed with the pET-11a plasmid which contained either wild type *ompR*, C67S, or K105R. Because ampicillin is toxic to this strain (Davies, J. and P. Reeves, 1975), a kanamycin cassette was subcloned into the *PstI* site of the ampicillin resistance gene in pET-11a-*ompR*). Cells were cultured for 6 hours at 37°C in 10 ml of LB, then harvested, quick-frozen in a dry ice methanol bath and resuspended in 30 mM TrisHCl pH 8.0, 20% sucrose (w/v). Lysis was initiated by addition of 25 μg/ml lysozyme followed by a 60 second

sonication. Intact cells were pelleted for 15 minutes at 2000xg, the supernatant was removed and centrifuged at 15,000 rpm (J2-21 Beckman) for 60 minutes. The pellet containing the cell envelope fraction was resuspended in sample buffer, loaded onto a 12% polyacrylamide-urea gel and electrophoresed for 2 hours at RT (130V).

Fluorescence anisotropy measurements. The DNA binding assays were performed at RT by titrating serial dilutions of protein into a binding solution containing (mM): 5 Na_2HPO_4/NaH_2PO_4 pH 7.4, 50 NaCl, 5 $MgCl_2$, 0.05% Tween 20, 25 μg/ml poly d(I-C), 56 μg/ml bovine serum albumin, and 2-8 nM fluoresceinated oligonucleotide (Sequences depicted in Table I, results). Samples were excited at 490 nm and emission was measured at 530 nm on a PanVera Beacon Fluorescence Polarization System. Binding reactions were incubated in the fluorimeter for 30 s and four measurements were taken at 10 s intervals after each protein addition. 5′ fluoresceinated oligonucleotides in which the upper strand of the DNA was labeled with fluorescein were purchased HPLC purified (Genosys Biotechnologies). Annealing of the complementary fluoresceinated and non fluoresceinated strands (1:1.2 ratio, respectively) was accomplished by heating at 90°C for 5 minutes followed by slow cooling to room temperature. The purity of the double stranded DNA was confirmed by native PAGE (greater than 95%).

Data Analysis. A model in which the K_d values represent the protein concentration at the half-maximal change in anisotropy was used. Curves

were fit with a non-linear least squares regression analysis. $A-A_o = V_{max}$ $[P]/(K_d + [P])$, where [P] signifies protein concentration, $V_{max,}$ the maximal change in anisotropy and $K_{d,}$ the apparent dissociation constant. A nonspecific component, a[P] + b (a and b are constants), was included to account for the linear change in anisotropy at high protein concentrations where appropriate.

Circular Dichroism. For secondary structure measurements, purified OmpR protein was dialyzed in a buffer containing 15 mM potassium phosphate, pH 7.5, 200 mM NaF at 4^0C for at least 6 hours. N-lauryl maltoside (Sigma) was added to a final concentration of 0.02% (w/v). The protein concentration was initially determined by absorbance measurements at 280 nm using an extinction coefficient of 13490 M^{-1} and confirmed by amino acid analysis. CD spectra were measured at protein concentrations ranging from 0.07 mg/ml to 1.4 mg/ml on a Jasco J500A spectropolarimeter using 0.01, 0.05, or 0.1-cm path length cells (Helma). The instrument was calibrated with (+)-10-camphor-sulfonic acid ($\Delta\varepsilon$ = +2.37 M^{-1} cm^{-1} at 290.5 nm and -4.95 at 192.5 nm). The data were collected on an IBM/PC-AT using the IF-500 interface and software provided by Jasco. Spectra and buffer base lines were the average of 8 scans recorded at 0.1-nm intervals, with a scanning rate of 10nm/min and a 2 s time constant. Both spectra and buffer baselines were smoothed using Jasco software and then the baseline was subtracted from the smoothed

spectra. CD spectra were deconvoluted for secondary structure content using variable selection methods (Compton, L. A. *et al.*, 1986; Manavalan, P. *et al.*, 1987). Combinations of a set of 33 basis spectra (kindly provided by W. Curtis Johnson, Jr., Oregon State University) were searched to find those offering the best fit using criteria as previously defined (Compton, L. A. *et al.*, 1986) Secondary structure values from combinations meeting these criteria were averaged for each set of spectra. The standard error for each secondary structure value was typically less than 0.1%.

Spectra measured in the presence of DNA are difference spectra in which the CD spectra of F1 DNA has been subtracted from a spectra of OmpR or OmpR-P bound to F1. OmpR and *ompF* DNA were mixed at an equal concentration of at least 6 μM to ensure that more than 90% of the OmpR would be bound to DNA. The spectra of OmpR-P typically contained a mixture of OmpR-P (30%) and unphosphorylated OmpR (70%), determined by separation on C4 as described in Methods.

Binding Assay using an Optical Biosensor. An IAsys optical biosensor from Fisons Technologies was used to measure affinities of OmpR for F1, C1 and F1+F2 oligonucleotides. In this assay, OmpR protein (50 nM - 5 μM) was added to a carboxy-methyl dextran cell with biotin-labeled DNA attached to its surface via a streptavidin linkage. In order to monitor OmpR binding to DNA, changes in refractive index at the cell surface were measured over time. A microstirrer operating at 60 revolutions per second mantained a

homogeneous solution and measurements were taken at 0.2 second intervals.

K_d values were obtained using software provided by Affinity Sensors. Plots of on rates versus protein concentration were linearly fit assuming biphasic association. The calculated gradient was equal to the association rate and the y-intercept was equal to the dissociation rate.

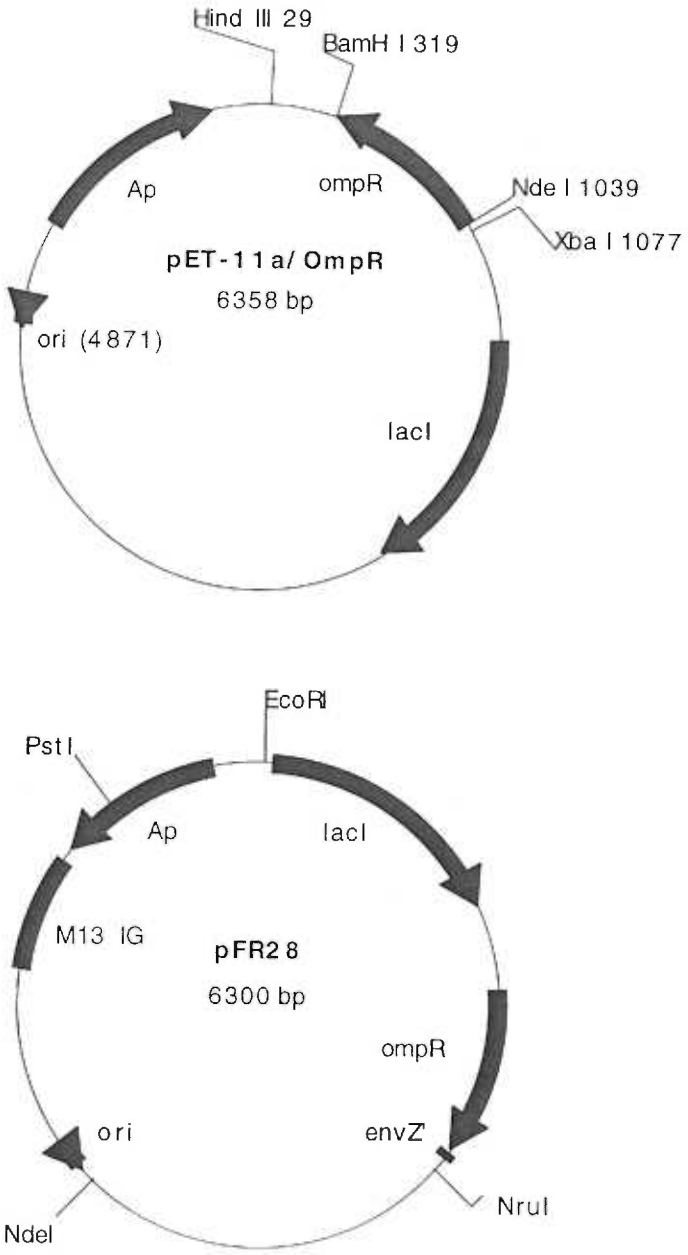

Figure 1. pFR28 and pET-11a-OmpR are both pBR322 based plasmids. pFR28 contains an M13 packaging signal, *lacI*^{Q} and the *ompB* operon under control of both its own and the *lac* promoter. pET-11a-OmpR has the *ompR* gene cloned into the NdeI and BamHI sites of pET-11a (Novagen). *ompR* expression is under control of the T7 RNA polymerase promoter.

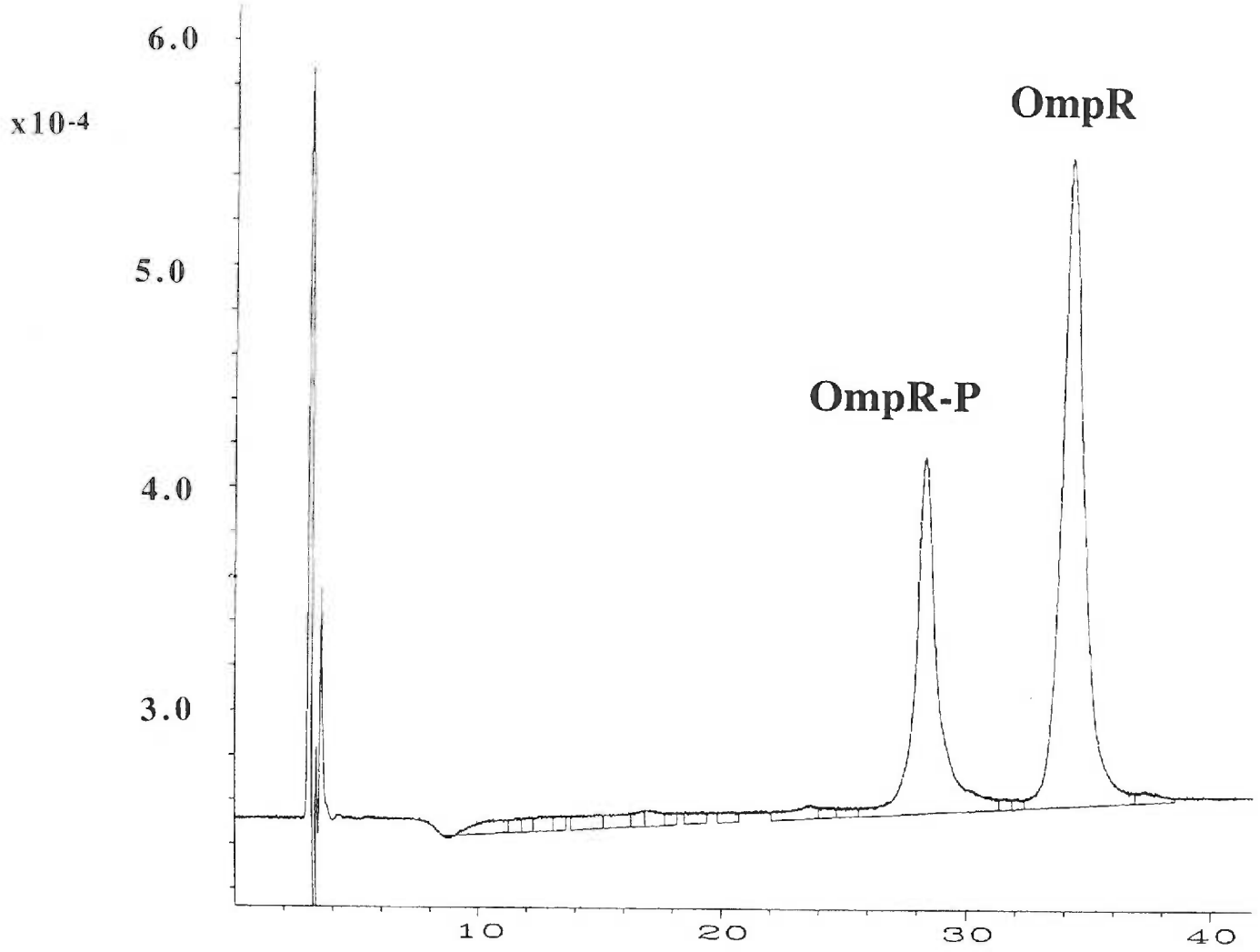

Figure 2. Separation of OmpR and OmpR-P by high performance liquid chromatography. The elution buffers were A, 20% and B, 60% acetonitrile in 0.1% trifluoroacetic acid. OmpR-P elutes as the earlier of two peaks from a C4 reverse phase column. Areas under the peaks were integrated to calculate the proportion of OmpR-P in samples treated with acetyl phosphate (C4 analysis done by C. Head).

Results

Phosphorylation of OmpR enhances its affinity for the ompF and ompC promoter regions. Based on footprinting data (Huang, K. and M. Igo., 1996; Harlocker, S. *et al.*, 1995), the *ompF* promoter contains three OmpR binding sites centered around -100/-40 upstream from the *ompF* transcriptional start site, designated F1, F2 and F3 (see Figure 3, introduction). Previous studies on this region have used gel shift assays in which the concentration of OmpR-P was not determined. I wanted to measure the binding constants in solution in order to directly test the simple affinity model. For direct measurements of DNA binding, I used fluorescence anisotropy in order to measure the relative affinities of OmpR and OmpR-P to oligonucleotides corresponding to the different OmpR binding sites. A binding curve of OmpR and OmpR-P to the F1 region of *ompF* is shown in Figure 1. The apparent equilibrium dissociation constant (K_d) for the OmpR:F1 complex is 180 nM, but when the curves are repeated with OmpR-P, the K_d decreases to 7 nM. Duplicate curves were reproducible (data not shown). Thus, the K_d value for the OmpR-P:F1 complex is approximately 20 times greater than the unphosphorylated OmpR:F1 complex, and confirms the earlier observations of Huang *et al.*, that phosphorylation of OmpR increases its affinity for DNA. A summary of my studies on the *ompF* promoter is shown in Table 2a.

It has previously been shown by gel shift analysis that OmpR is

incapable of binding to the F2 and F3 regions of *ompF* in the absence of F1 (Huang, K. *et al.*, 1996). However, if F1 was attached to F2, OmpR could bind to F2, as evidenced by an additional shift in the observed assay. To determine the affinity of OmpR at this double site, binding of OmpR and OmpR-P to F1+F2 DNA was measured (Figure 2). Apparent K_d values of OmpR and OmpR-P for this site were 205 nM and 14 nM, respectively. These values are essentially identical to the affinity of OmpR for the isolated F1 region. Thus it is not possible to observe two discrete binding steps for OmpR by fluorescence anisotropy.

Figure 3 compares binding of OmpR and OmpR-P to the F1+F2+F3 region of *ompF*. Again, apparent Kd values were similar to those for the F1 region, at 140nM and 15nM for OmpR and OmpR-P, respectively. Whenever the F1 site is present, it appears to convert the *ompF* promoter to high affinity.

Although binding at F2 and F3 was not observed in the gel shift assay in a previous study, I wanted to determine whether OmpR could bind to these sites independently. To test this possibility, an oligonucleotide representing the F2+F3 region of OmpR was used in binding experiments (Figure 4). Both OmpR and OmpR-P were able to bind to this site, albeit with lower affinity than observed for the F1 region alone. The K_d value of OmpR for F2+F3 was 1800 nM and for OmpR-P, 91 nM. These affinities are approximately 10 fold lower than those for F1. The F2 and F3 regions were

also used separately in binding assays to determine whether the affinity of OmpR for the individual sites was comparable to its affinity for F2+F3. OmpR and OmpR-P had similar affinities for F2 and F3 (Table 2a) and K_d values were only slightly higher than those measured for F2+F3. This indicates that OmpR-P (and OmpR) can bind to these sites in the absence of F1 and that the gel shift assay was not able to resolve this binding (Huang, K. and M. Igo, 1996).

Figure 5 represents a comparison of OmpR and OmpR-P binding to the C1 region of the *ompC* promoter. The simple affinity model predicts that this site should be low affinity. The K_d value for the phosphorylated complex is 2 nM and 40 nM for the unphosphorylated complex. In this case, the K_d values for the phosphorylated and unphosphorylated forms of OmpR differ by approximately 20 fold and the affinity of both OmpR and OmpR-P at the C1 site is even higher than at the F1 site. This result suggests that OmpR-P would not be able to discriminate between F1 (with a K_d of 7 nM) and C1 (K_d 2-5 nM).

The DNA binding activity of many DNA binding proteins is sensitive to the salt concentration in the assay. In the case of OmpR, increasing the NaCl concentration from 50 mM to 150 mM markedly decreases its affinity for both F1 and C1 sites. At F1, this results in a two-fold decrease in affinity (Table 2b). In Figure 6, the affinities of unphosphorylated OmpR for C1 at 50

mM and 150 mM NaCl are compared, and the comparable curves for OmpR-P are shown in Figure 7. While increasing the NaCl concentration affects both sites in the same direction, it is interesting to note the following differences: At C1, the affinity for OmpR-P is nearly identical to that measured at 50 mM NaCl, yet the K_d for unphosphorylated OmpR is increased 10-fold. In contrast, measurements with F1 made in the presence of 150 mM NaCl affected the K_d for both OmpR and OmpR-P approximately 2-3 fold.

The C-terminal portion of OmpR (OmpRc) reportedly binds the *ompF* and *ompC* promoter regions with a greater affinity than unphosphorylated OmpR (Harlocker, S., 1996). To confirm this observation, binding of OmpRc to C1, F1 and F1+F2+F3 was assayed by fluorescence anisotropy. In the case of C1 and F1, an almost negligible change in polarization was observed as the concentration of OmpRc was increased. It is possible that an interaction between OmpRc and DNA would not be detected by this method because OmpRc (12 kDa) may not be large enough to cause a change in the anisotropy of the DNA. However, a change in anisotropy was detected when OmpRc was titrated into a solution containing F1+F2+F3. The apparent K_d value for complex formation was 50 nM, which lies between the values measured for OmpR and OmpR-P binding to this region. Since F1+F2+F3 has a larger mass than either F1 or C1 (45,000 g/mol as opposed to 15,000 g/mol for F1 or C1), it should give rise to a greater change in total anisotropy upon binding of OmpRc, if each promoter region is bound by OmpR. Alternatively, it is

possible that OmpRc binds to F1+F2+F3 but not to F1 or C1.

Response regulators in the same subfamily as OmpR (e.g. PhoB, VirG) all have significant similarity in their primary sequences and presumably have the same overall structure as OmpR, including the winged helix-turn helix (HTH) DNA binding motif. Each member of this group regulates a specific set of target genes *in vivo*, probably because of subtle differences in their DNA binding domains. To verify that OmpR interacts specifically with its promoter regions *in vitro*, binding of phosphorylated PhoB to F1+F2+F3 was assayed. The K_d value measured for this interaction was 1200 nM, approximately 100 fold greater than the value measured for OmpR-P.

Genetic studies have suggested that OmpR interacts with the C-terminal domain of RpoA (α-CTD) *in vivo* (Slauch, J. M. and T. J. Silhavy, 1991; Sharif, T. R. and M. Igo, 1993). I therefore wanted to test the effect of adding α-CTD to our fluorescence anisotropy assay. I used the C1 site for this purpose, since it has the highest affinity for OmpR and OmpR-P. When OmpR-P was titrated into a solution containing α–CTD and C1 DNA, no change in anisotropy was observed (see Discussion section for possible explanations for this result).

Two mutants of OmpR, K105R and C67S, were assayed for their ability to bind C1 DNA. Only the unphosphorylated forms were used, because both mutants are not phosphorylated by either acetyl phosphate or by EnvZ115 (a

truncated derivative of EnvZ that retains its kinase activity, Igo, M. and T. J. Silhavy, 1988). The highly conserved lysine at position 105 was mutated because a homologous mutation in the chemotactic response regulator CheY results in a protein that dephosphorylates more slowly than wt-CheY (Lukat, G. S. *et al.*, 1991). K105R binds to the C1 region of *ompC* with the same affinity as wt-OmpR. The K_d values are 42 nM for K105R and 40 nM for wt-OmpR. C67S also binds to DNA, although with a lower affinity than wt-OmpR. The K_d value for the C67S:C1 complex is 117 nM, about three-fold lower than the affinity of wt-OmpR for this region. Cysteine 67 is the only cysteine in OmpR and it was changed to serine because of the difficulty in concentrating OmpR for crystallization trials.

The affinity of K105R for two regions of the *ompF* promoter was also measured. Its affinity for the F1 region is 154 nM and for F1+F2+F3 is 190 nM. Again these values are within the range of apparent K_d values observed for wt-OmpR:DNA complexes.

Binding of OmpR to F1 and C1 measured by an optical biosensor. The affinity of OmpR for the F1 and C1 promoter regions was measured in the presence of 150 mM NaCl. The K_d values for unphosphorylated OmpR binding to F1 and C1 DNA were 320 nM and 280 nM respectively. These values agree well with those obtained using fluorescence anisotropy. Binding to the F1+F2 region of *ompF* was also measured using this method and

yielded a K_d value of 220 nM. However, this method was not useful for measuring OmpR-P binding to DNA, because the change in refractive index between the binding buffer and the buffer containing the protein was too great.

Circular dichroism of OmpR. Circular dichroism spectra of OmpR were measured and solved in order to determine the secondary structure content of OmpR. The average secondary structure content of OmpR is approximately 27% α-helix, 25% β-strand, 19% β-turn and 29% random coil. A representative spectra is shown in Figure 8. The secondary structure content from CheY, an N-terminal homologue of OmpR, was combined with secondary structure information from the crystallization data on the C-terminal domain of OmpR, to compare it to my results on the intact OmpR protein. The combined results gave a significantly greater portion of α-helix (37%) than that of intact OmpR (27%). OmpR spectra were then measured at concentrations ranging from 0.07 - 1.1 mg/ml (2.5 - 40 μM) in order to determine whether there were any concentration-dependent changes in its secondary structure. The results are summarized in Figure 9. A trend was observed in which the proportion of β-strand decreased and α-helix increased as the concentration of OmpR increased.

Phosphorylation of a protein can lead to its activation via a global change in structure. To examine this possibility, CD spectra of the

unphosphorylated and phosphorylated forms of OmpR were measured and compared. There was no significant difference between the secondary structures of these two forms of the protein. One difficulty in this approach, however, is that the proportion of OmpR that can stably remain phosphorylated upon treatment with acetyl phosphate is approximately 30%. Therefore, only a drastic change in secondary structure would be observable by this method.

DNA binding proteins sometimes change conformation upon binding to DNA. Difference spectra of OmpR and of OmpR-P in the presence and absence of F1 DNA were measured using circular dichroism in order to compare the secondary structure of OmpR when it was bound to DNA. Again, no significant difference was observed in the secondary structures of these two forms of the protein, indicating that there is no global change in the secondary structure of OmpR upon binding to DNA.

Since single point mutations in a protein can sometimes lead to global structural changes, I measured their CD spectra to verify that the secondary structures of K105R and C67S were not affected by the mutation. In each case, the secondary structure was similar to that of wt-OmpR (data not shown).

The stability of the mutants compared to wt-OmpR was examined by monitoring intrinsic fluorescence versus temperature. The melting temperature of the proteins was the point at which the half-maximal change in fluorescence was observed. Wt-OmpR, K105R and C67S all melted at the

same temperature, 59°C, indicating that the point mutations did not alter the stability of OmpR. A representative plot of fluorescence versus temperature is shown in Figure 10.

To address whether OmpR exists as a monomer or dimer in solution, dynamic light scattering of both the phosphorylated and unphosphorylated forms were measured. At 5 mg/ml (180 μM), OmpR has an apparent molecular weight (MW) of 43 kDa. A solution of approximately 30% OmpR-P (and 70% OmpR) has a MW of 66 kDa. Bovine serum albumin, a 67 kDa monomer *in vivo*, has an apparent MW of 85 kDa at 5 mg/ml by this method. Results from analytical ultracentrifugation at 3 mg/ml yield an apparent MW of 45 kDa for OmpR and 54 kDa for OmpR-P (Kenney, L. J., unpublished data). At lower concentrations, OmpR appears to exist exclusively as a monomer.

Another approach to test for dimer formation was to pass OmpR and OmpR-P (3 mg/ml) over a gel filtration column. The absorbance at 280 nm was monitored, and a single peak eluting from the column at ~30 kDa was observed for both forms of OmpR (data not shown). Gel filtration of K105R resulted in a single peak eluting at the same position as that of wt-OmpR. In the case of the closely related PhoB-P protein, however, dimer formation is observed at 2 mg/ml by HPLC (McCleary, W., 1996).

To investigate the effects of phosphorylation and DNA binding on OmpR conformation, trypsin cleavage patterns of OmpR and OmpR-P in the

presence and absence of F1 DNA were compared (Fig 11). Several types of global structural changes, such as movement about a hinge, are often reflected by changes in protease cleavage patterns. Fragments at approximately 4 and 6 kDa (by SDS-PAGE), were observed in the presence of DNA, but not in its absence, by SDS-PAGE. Also, the rates at which digestion proceeded varied markedly. OmpR was digested most rapidly, followed by OmpR-P, OmpR bound to F1 DNA and finally OmpR-P bound to DNA. Sensitivity to proteases often indicates that a particular region is solvent-exposed or that it has a high degree of random structure. Trypsin digestion rates of K105R both with and without F1 DNA were similar to those of wt-OmpR +/- DNA.

The porin phenotypes of the OmpR mutants were examined. The strain MH1160 has a small in-frame deletion in *ompR* and is therefore *ompR*$^-$, but *envZ*$^+$ (Sarma, V. and P. Reeves, 1977). MH1160 was transformed with the pET-11a plasmid encoding genes for either *wt-ompR*, *ompR-K105R* or *ompR-C67S*. In all cases, both the OmpF and OmpC porins were produced at low osmolarity (Fig 12), whereas at high osmolarity *ompF* expression was repressed and OmpC production was increased. Thus, in this assay, there was no difference in porin expression between the mutants and wt-OmpR. Although the mutants are not phosphorylated *in vitro*, they were able to respond to changes in osmolarity in this system.

Table I. Oligonucleotides used in this study. Regions in bold represent promoter regions. (Huang, K., *et al* 1996; Maeda, S. and T. Mizuno, 1990)

OLIGO	*ompF* region	sequence of oligonucleotide
F1	-100/-81	ggctttA**CTTTTCCTTACATATT**c
F2	-79/-56	agcttT**CTTTTTGAAACCAAATC**tttaagct
F3	-59/-36	agctttA**TATCTTTGTAGCACTTTC**acggagct
F1-F2	-102/-56	attttA**CTTTTGGTTACATATTT**ttT**CTTTTTGAAACCAAATC**ttT**A**
F2-F3	-79/-36	acgtT**CTTTTTGAAACCAAATC**ttT**ATCTTTGTAGCACTTTC**acgg
F1-F2-F3	-102/-36	attttA**CTTTTGGTTACATATTT**ttT**CTTTTTGAAACCAAATC**tt T**ATCTTTGTAGCACTTTC**acgg
	ompC region	
C1	-107/-72	tcccttgcatttA**CATTTTGAAACATCTAT**agcgat

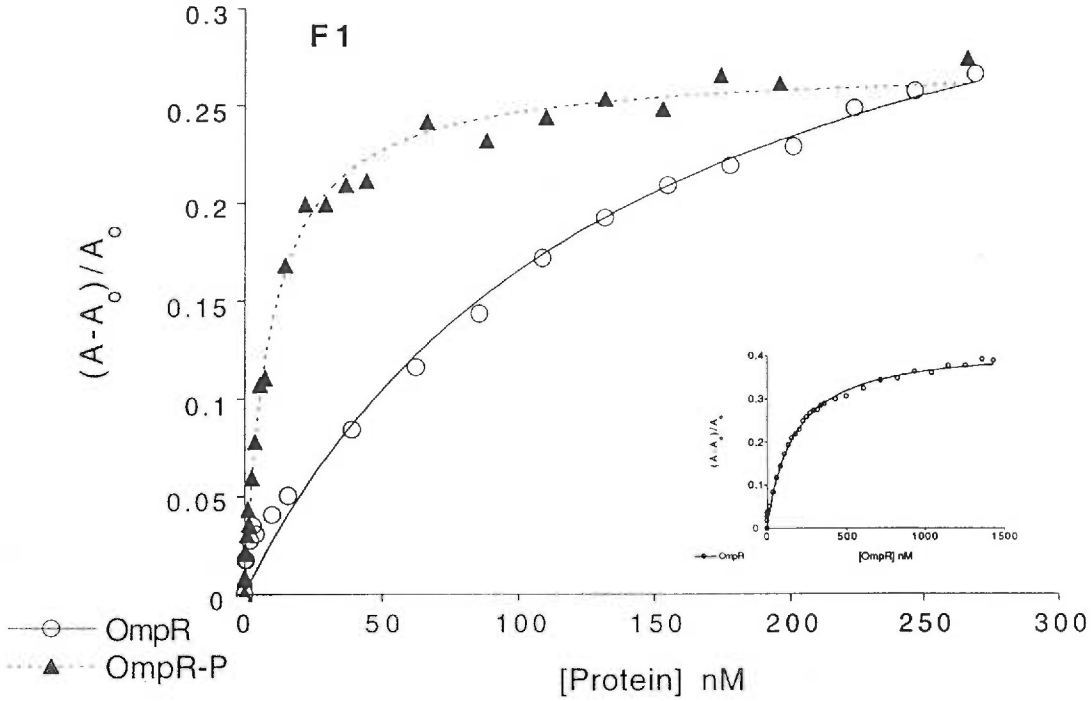

FIGURE 1. Binding curve of OmpR and OmpR-P to F1 DNA using fluorescence anisotropy. The normalized change in anisotropy is plotted against OmpR or OmpR-P concentration. Inset shows the full-scale curve of OmpR binding to F1 DNA. Ao is the anisotropy value of F1 in the absence of protein and A is the measured anisotropy value after addition of OmpR. Binding assays were done at RT by titrating serial dilutions of protein into a binding solution containing (mM): 5 Na_2HPO_4/NaH_2PO_4 pH 7.4, 50 NaCl, 5 $MgCl_2$, 0.05% Tween20, 25µg/ml poly d(I-C), 56 µg/ml bovine serum albumin, and 2 nM F1 fluoresceinated DNA. Samples were excited at 490 nm and emission was measured at 530 nm.

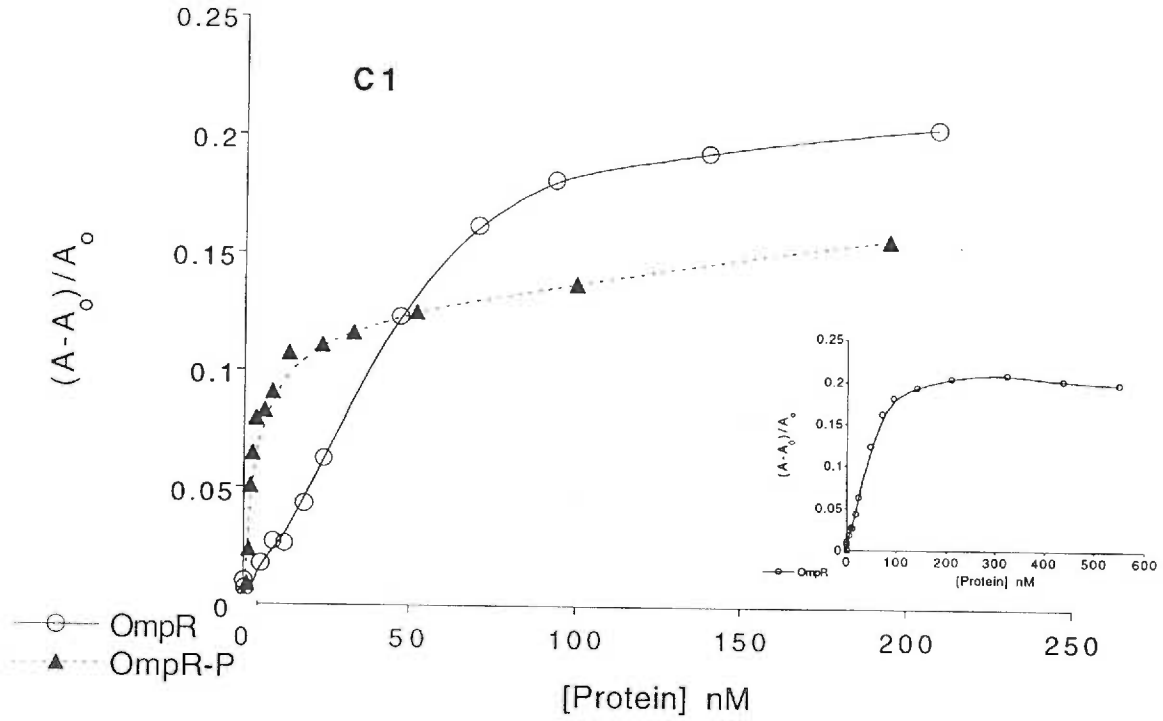

FIGURE 2. Binding curve of OmpR and OmpR-P to C1 DNA using fluorescence anisotropy. The normalized change in anisotropy is plotted against OmpR or OmpR-P concentration. Inset shows the full-scale curve of OmpR binding to C1 DNA. Conditions are described in Figure 1 except that 8 nM of fluoresceinated C1 DNA was used.

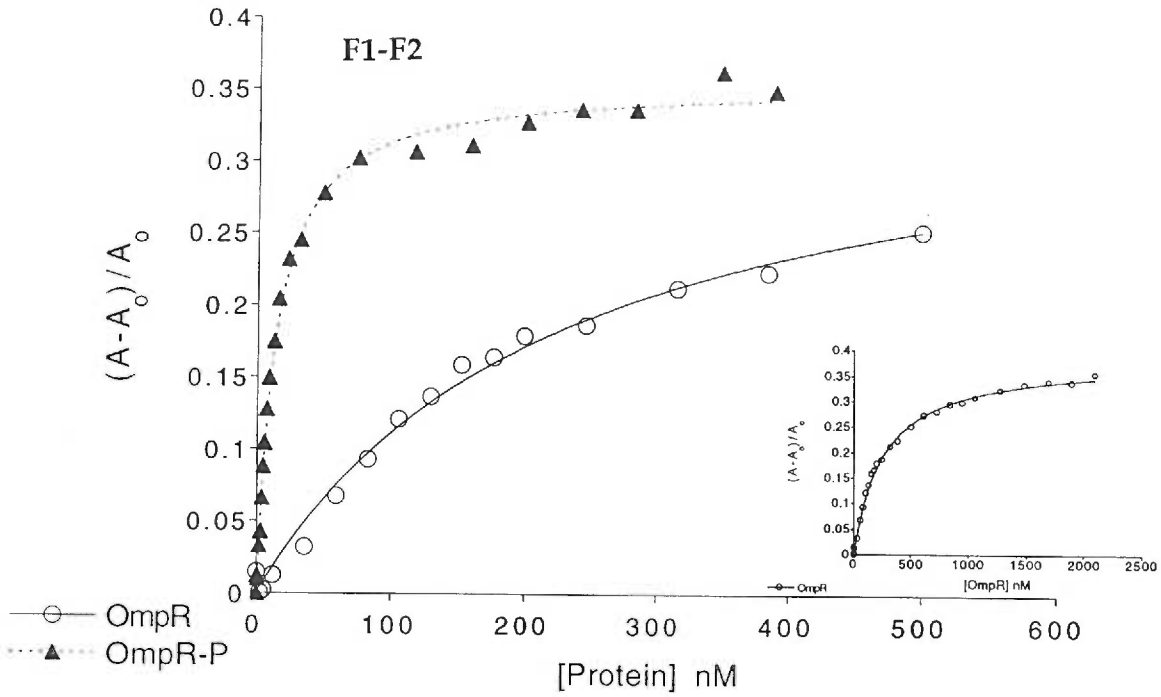

FIGURE 3. Binding curve of OmpR and OmpR-P to F1-F2 DNA using fluorescence anisotropy. The normalized change in anisotropy is plotted against OmpR or OmpR-P concentration. Inset shows the full-scale curve of OmpR binding to F1-F2 DNA. Conditions are described in Figure 1 except that 2 nM of fluoresceinated F1-F2 DNA was used.

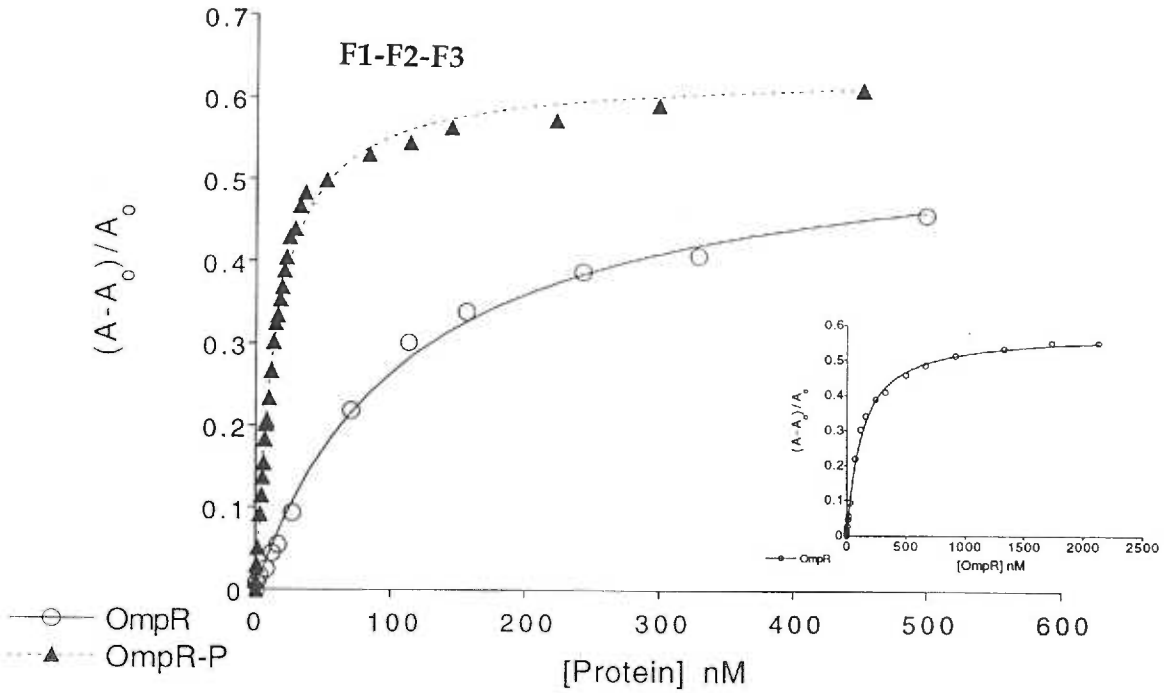

FIGURE 4. Binding curve of OmpR and OmpR-P to F1-F2-F3 DNA using fluorescence anisotropy. The normalized change in anisotropy is plotted against OmpR or OmpR-P concentration. Inset shows the full-scale curve of OmpR binding to F1-F2-F3 DNA. Conditions are described in Figure 1 except that 2 nM of fluoresceinated F1-F2-F3 DNA was used.

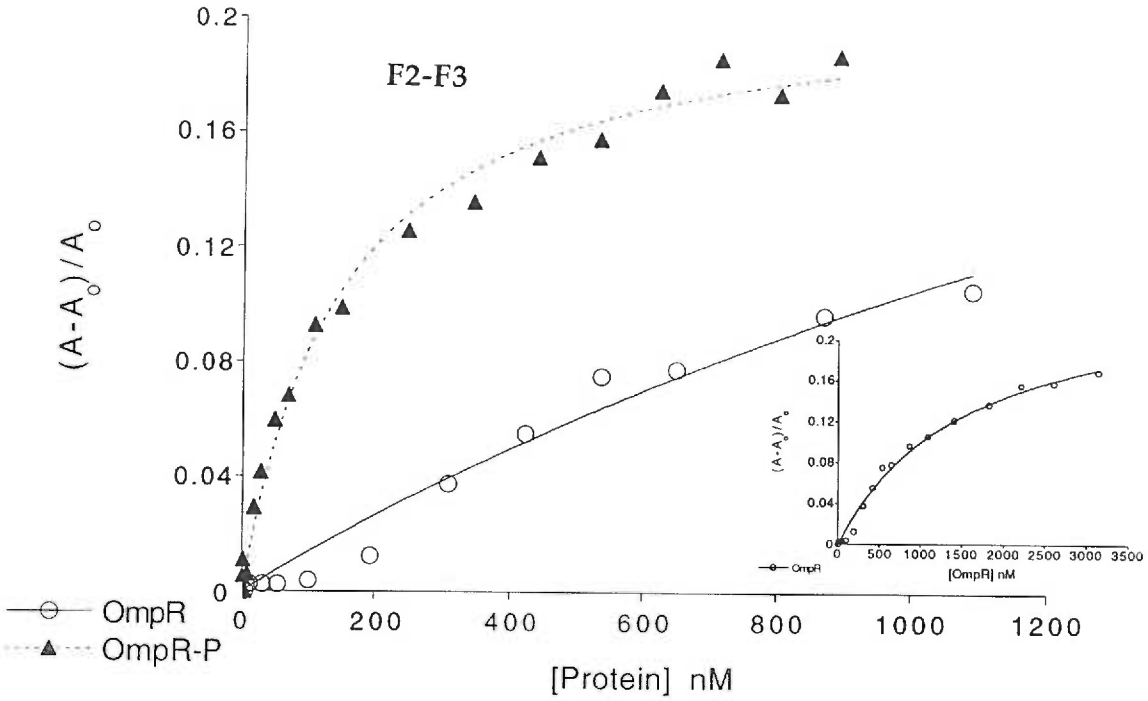

FIGURE 5. Binding curve of OmpR and OmpR-P to F2-F3 DNA using fluorescence anisotropy. The normalized change in anisotropy is plotted against OmpR or OmpR-P concentration. Inset shows the full-scale curve of OmpR binding to F2-F3 DNA. Conditions are described in Figure 1 except that 3 nM of fluoresceinated F2-F3 DNA was used.

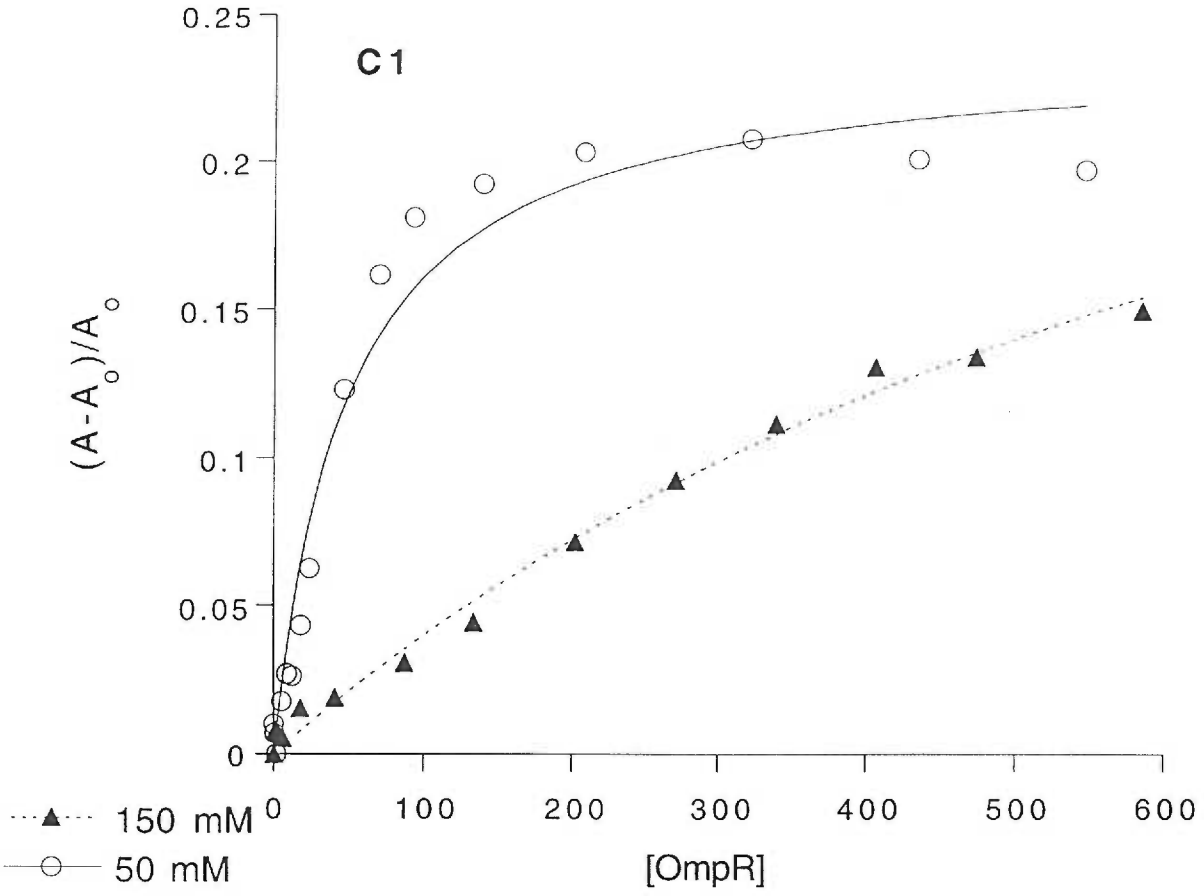

FIGURE 6. Binding curve of OmpR to C1 DNA at 50 mM and 150 mM NaCl using fluorescence anisotropy. The normalized change in anisotropy is plotted against OmpR concentration. Conditions are described in Figure 1 except that the high salt binding buffer contained 150 mM NaCl and 10 mM Na_2HPO_4/NaH_2PO_4 pH 7.4.

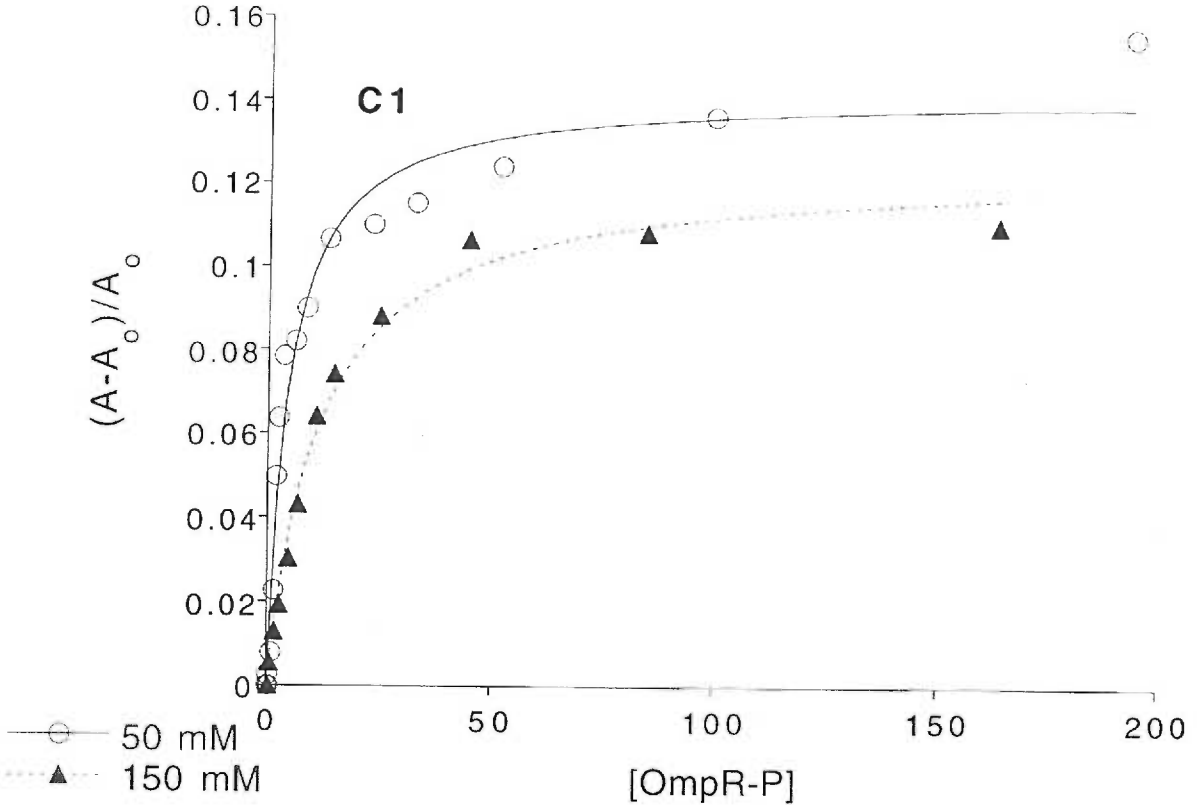

FIGURE 7. Binding curve of OmpR-P to C1 DNA at 50 mM and 150 mM NaCl using fluorescence anisotropy. The normalized change in anisotropy is plotted against OmpR-P concentration. Conditions are described in Figure 1 except that the high salt binding buffer contained 150 mM NaCl and 10 mM Na_2HPO_4/NaH_2PO_4 pH 7.4.

Table 2a Dissociation constants of OmpR and OmpR-P in 50 mM NaCl

	Kd	
Site	OmpR	OmpR-P
F1	181 +/- 25 nM	7.1 +/- 2.8 nM
C1	40 +/- 14 nM	2.1 +/- 1.5 nM
F2	1400 nM*	140 nM*
F3	1400 nM*	140 +/- 64 nM
F1+F2	205 +/- 8 nM	14 +/- 5 nM
F2+F3	1800 +/- 300 nM	91 +/- 3 nM
F1+F2+F3	140 +/- 28 nM	15 +/- 6 nM

Table 2b Dissociation constants of OmpR and OmpR-P in 150 mM NaCl

	Kd	
Site	OmpR	OmpR-P
F1	390 +/- 160 nM	32 nM*
C1	400 nM*	5 nM*

*Correlation coefficient, R, is greater than 0.95, n=1

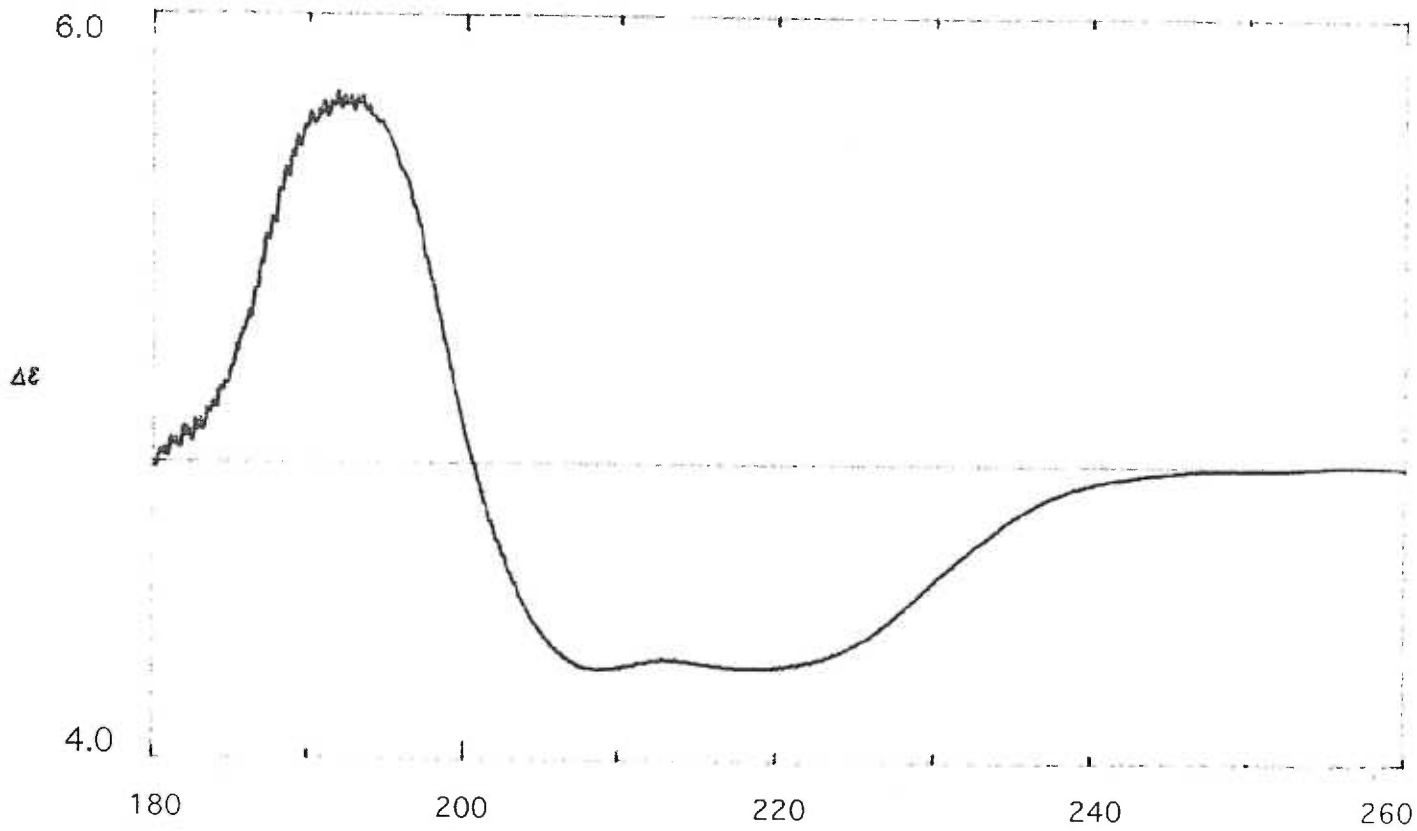

Figure 8. Circular dichroism spectrum of OmpR (12 μM) at 20°C. Wavelength (nm) is represented along the x-axis and change in extinction coefficient (Δε) along the y-axis.

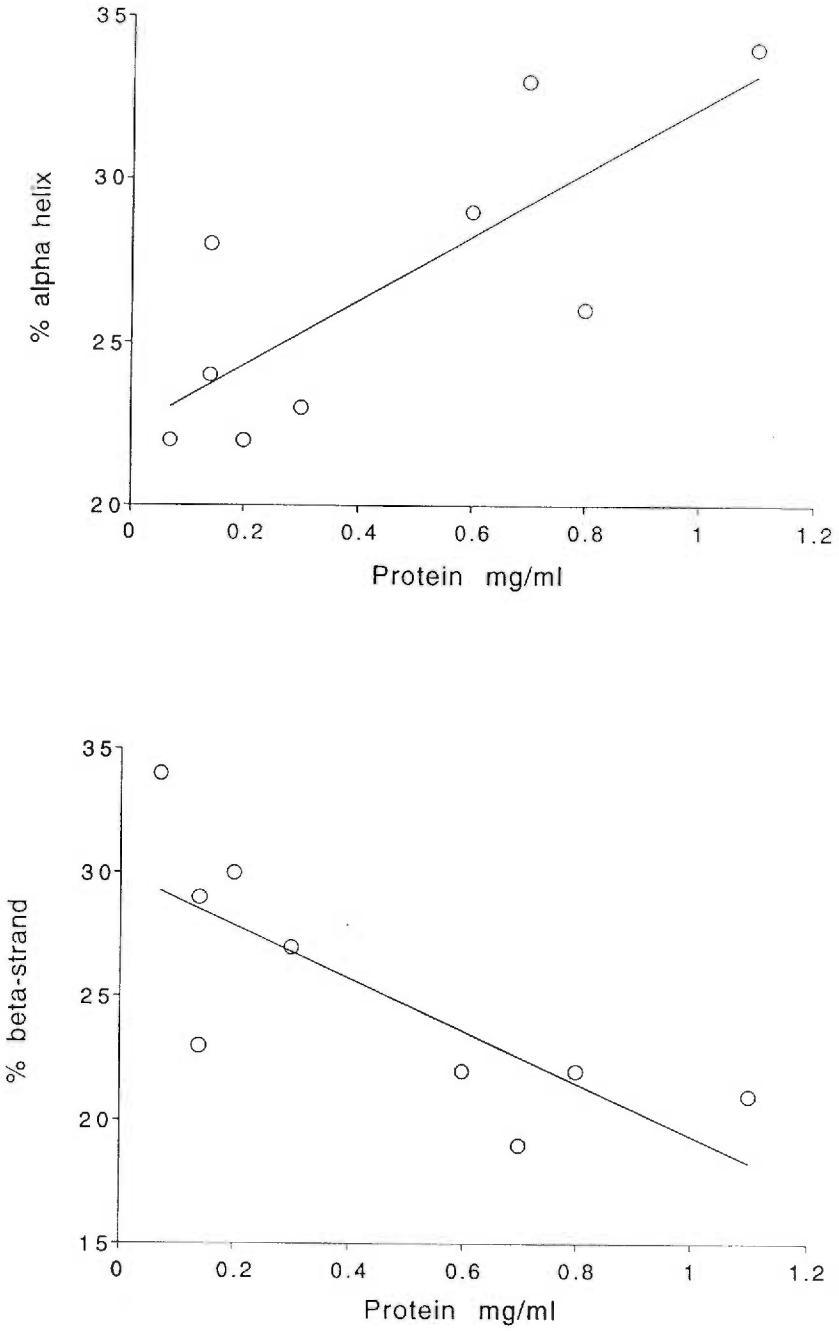

Figure 9. Top: α-helix content is plotted versus OmpR concentration. Bottom: β-strand content is plotted versus OmpR concentration.

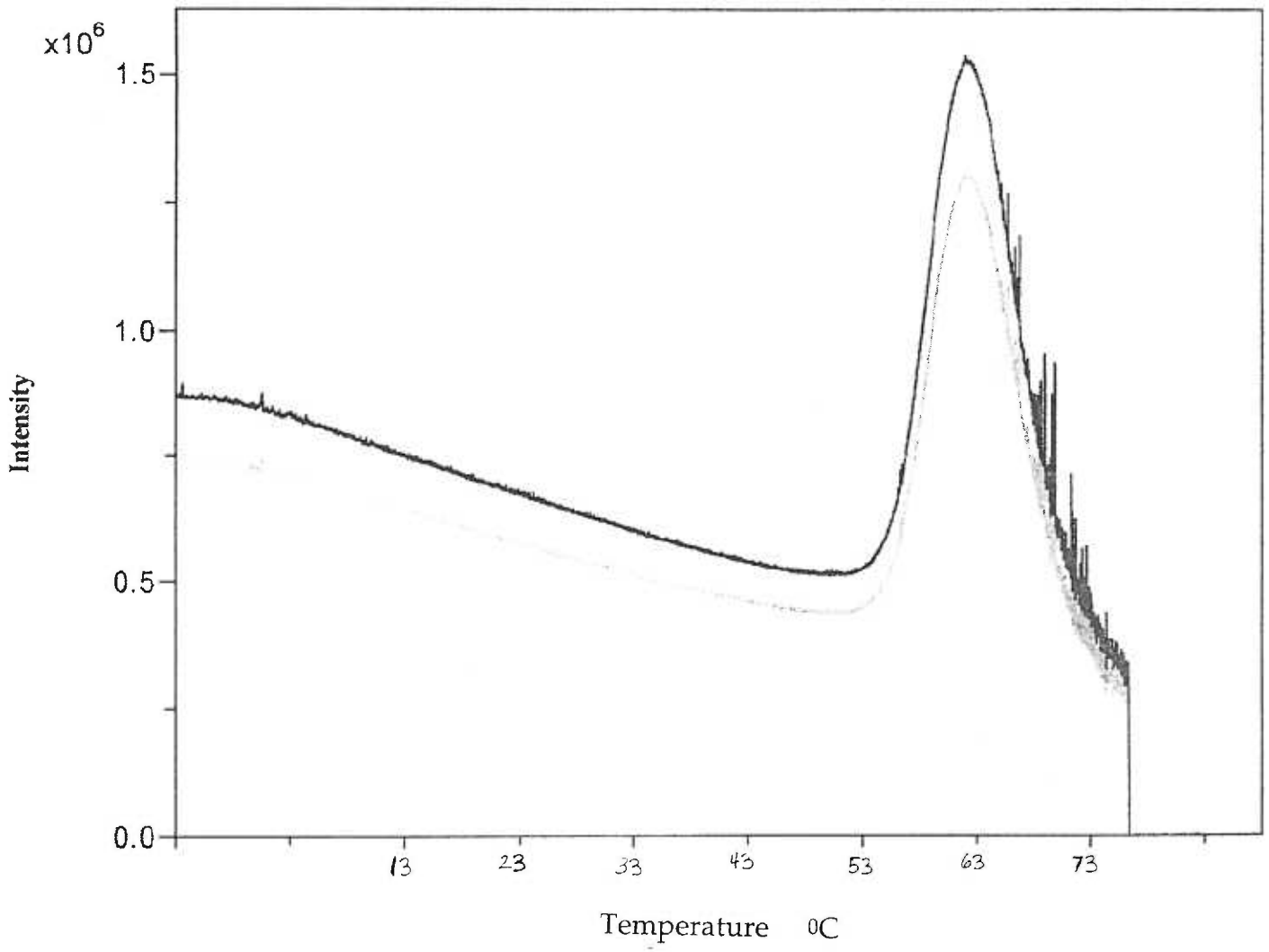

Figure 10. Melting curve of wt-OmpR monitored by intrinsic fluorescence. Intensity of fluorescence is plotted against temperature (°C). Temperature change was 0.02°C/s (1.2°C/min). Excitation wavelength was 295 nm and emission was monitored at 335 nm.

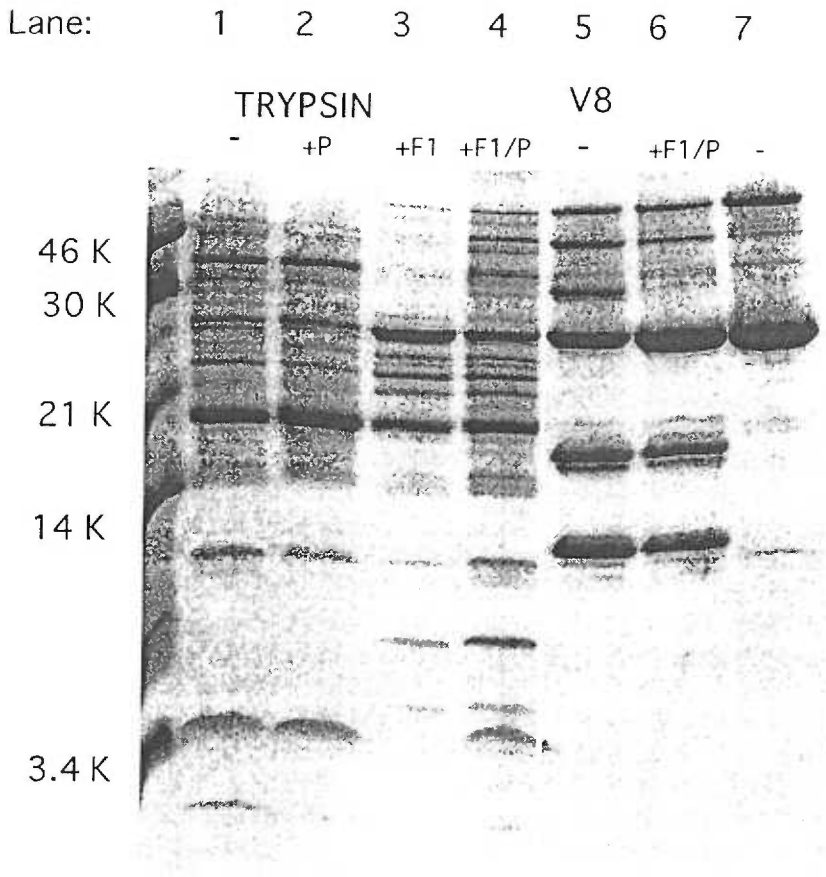

Figure 11. Protease digests of OmpR. OmpR (15 ug) was incubated with protease (100:1 w/w) for 12 minutes at 37° C. Lane 1 is a trypsin digest of OmpR, lane 2, is of OmpR-P, lane 3 is OmpR bound to F1 DNA, and lane 4 is OmpR-P bound to F1 DNA. Lanes 5 and 6 are V8 protease digests of OmpR and of OmpR-P bound to F1 DNA. Lane 7 is a sample of undigested OmpR.

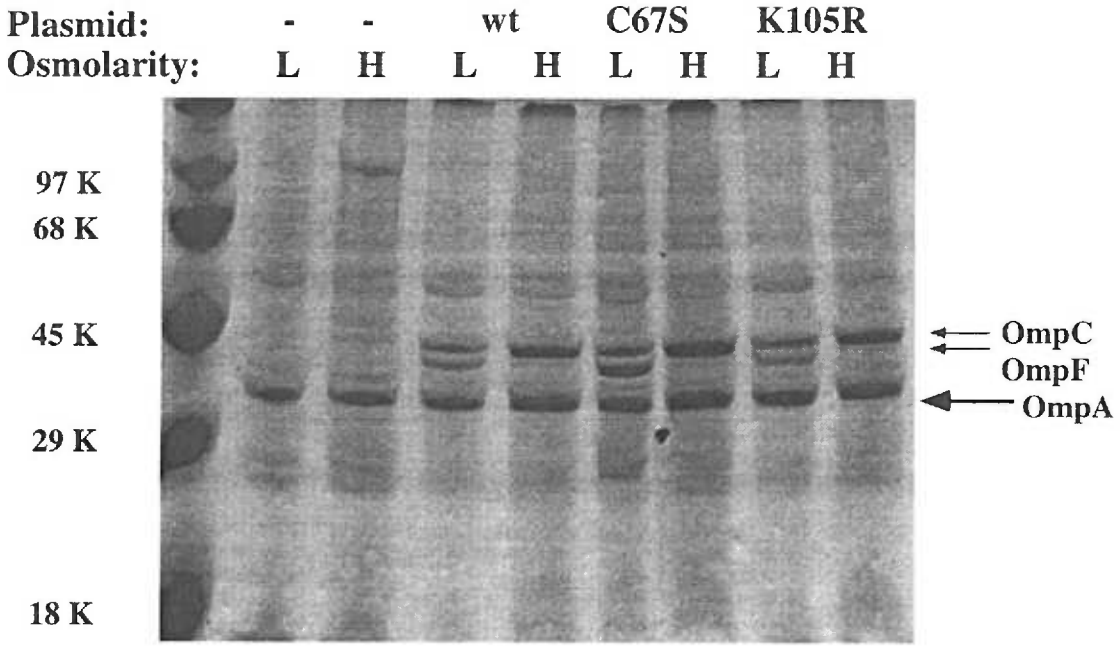

Figure 12. Porin phenotype of mutants. Samples were prepared as described in methods and separated on a 12% SDS polyacrylamide urea gel. Lanes 1 and 2 are outer membrane preparations of untransformed MH 1160 cells. Lanes 3 and 4 are preparations of MH 1160 cells transformed with pET-11a-*ompR*. Lanes 5 and 6 are of pET-11a-*ompR*-C67S in MH1160 and lanes 7 and 8 are MH1160 transformed with pET-11a-*ompR*-K105R. **L** = low osmolarity and **H** = high osmolarity.

Discussion

Relative binding affinities of OmpR and OmpR-P for the *ompF* and *ompC* promoter regions were measured to determine how phosphorylation affects binding to these promoters. Previous studies have used electrophoretic mobility shift assays and DNA footprinting to define the regions to which OmpR binds (Maeda *et al.*, 1990; Harlocker, S. *et al.*, 1995; Huang *et al.*, 1996). Gel shift data has also shown that OmpR-P has a greater affinity for its promoters compared to OmpR, but the interaction was never quantified. In the binding assays described in this work, phosphorylation enhanced binding of OmpR to its promoter sequences by 10 to 20-fold.

OmpR-P had the highest affinity for the C1 and F1 regions of *ompC* and *ompF*. This is in agreement with previous results using gel shift assays (Huang *et al.*, 1996). Apparent K_d values were higher for C1 (2 nM) than for F1 (7 nM), which was unexpected in the context of the current genetic model for porin regulation. The model predicts that OmpR-P has a higher affinity for promoter sites at *ompF* and a lower affinity for *ompC* sites. There are several possible explanations for this discrepancy, as discussed in the following paragraphs.

One possibility is that additional factors are necessary for transcriptional activation *in vivo* and that these factors act together to aid OmpR-P in distinguishing between the *ompF* and *ompC* promoters. Integration host factor (IHF), leucine repressor protein (Lrp), catabolite

activator protein (CAP), the nucleoid associated DNA binding protein (H-NS) and RNA polymerase (RNAP) have all been reported to interact with *ompF* (Ramani, N. *et al.*, 1992; Ernsting, B. *et al.*, 1992; Scott, N. and C. Harwood, 1980; Graeme, C. *et al.*, 1989; Slauch, J. M. and T. J. Silhavy, 1991)

At low osmolarity *in vivo*, OmpR-P may occupy the C1 site, but it may not bind at C2 and C3 until a higher osmolarity is reached. Activation of *ompC* transcription may require that all three sites be filled.

Studies using gel shift assays have shown that the presence of F1 is necessary for OmpR to bind to F2 and F3 (Huang *et al.*, 1996). Our results indicate that the presence of F1 confers high affinity binding on the nucleotide containing F2 and F3, but OmpR can bind to F2 and F3 in the absence of F1. The affinity of OmpR-P for both F2 and F3 is 145 nM, while the affinity for F2+F3 is 91 nM. These affinities are similar to that of unphosphorylated OmpR for F1, but about ten fold lower than the affinity of OmpR-P for F1. Unphosphorylated OmpR has a K_d value of approximately 1800 nM for F2, F3 and F2+F3. This affinity is quite low, and it is not surprising that a gel shift was not observed with these DNA fragments. However, the absence of a gel shift in the presence of OmpR-P (K_d = 91 nM) was most likely due to low levels of OmpR phosphorylated under the assay conditions. In addition, salt concentrations used in gel shift analysis (130 mM; Huang *et al.*) were higher than those used here and may have interfered with the electrostatic interactions between OmpR and DNA.

K_d values for F1+F2:OmpR-P (14 nM) and F1+F2+F3:OmpR-P (15 nM) were about two-fold greater than that for F1:OmpR-P (7 nM). These results indicate that the presence of F1 confers high affinity OmpR-P binding on the *ompF* promoter.

Increasing the NaCl concentration to 150 mM in binding assays resulted in an increase in the apparent K_d values of OmpR and OmpR-P for both F1 and C1. High NaCl concentration decreases protein-DNA affinities due to the electrostatic nature of their interaction. However, DNA binding proteins generally have a high affinity for DNA at 150 mM NaCl. Moreover, salt concentrations often exceed 150 mM inside a bacterial cell. This raises the possibility that OmpR (and OmpR-P) binding to its promoters, and therefore porin expression, is affected by salt concentration in addition to phosphorylation. However, since the affinity at both F1 and C1 was increased, this result does not alter the contradiction with the simple affinity model raised by the binding data presented in this work.

OmpR mutants K105R and C67S were both able to bind C1 DNA. K105R had the same affinity for C1 as unphosphorylated OmpR and C67S had a three-fold lower affinity. Since the secondary structure of C67S is similar to that of wt-OmpR, it would be expected to have a similar affinity for C1. The discrepancy may be explained by the observation that C67S tends to aggregate more readily than wt-OmpR, which would make less C67S available for DNA binding. In the wild type protein, C67 is located in the third α–helix of the N-

terminal domain. The related NarL and CheY proteins each have a leucine at the analogous position (Stock, A. M. *et al.*, 1989) indicating that the serine substitution may be too hydrophilic and cause destabilization of the α–helix .

The closely related PhoB protein has a 100-fold lower affinity when phosphorylated for F1+F2+F3 of *ompF* compared to OmpR-P. Both proteins likely have the same type of DNA binding motif, a winged HTH, but they each recognize different consensus sequences *in vivo* (Makino, *et al.*, 1986). The basis of this recognition is not understood but differences in a few key residues in the DNA binding domain may allow these proteins to distinguish one binding site from another.

OmpRc is reported to have a higher affinity for the *ompF* promoter than unphosphorylated OmpR (Harlocker, S., 1996). A binding assay using F1+F2+F3 and purified OmpRc supported this finding. The increase in affinity over that of OmpR was approximately two-fold but the assay was less reliable than that for full-length OmpR due to its smaller size (12 kDa). OmpRc caused a small change in the anisotropy of the fluorescein-labeled oligonucleotide. There was also a large non-specific component of binding at higher concentrations of OmpRc.

Genetic studies have shown that suppressors of *ompR* mutants unable to activate transcription *in vivo* map to the α-subunit of RNAP (*rpoA*; Slauch, J. M. and T. J. Silhavy, 1991; Sharif, T. R. and M. Igo, 1993). Mutations

restoring activity localize to the C-terminal domain of *rpoA* (α–CTD). This result suggested that RpoA and OmpR interact. To test this hypothesis, I included purified α–CTD in a binding assay of OmpR-P to C1 DNA. In the absence of α–CTD, the affinity of OmpR-P for this site was 2 nM. However, in its presence, no change in anisotropy was observed as OmpR-P was added. One explanation for this result is that α–CTD interacted with the DNA and prevented OmpR-P binding to F1, or that OmpR-P bound preferentially to the α–CTD in solution. There was no change in anisotropy upon addition of α–CTD to the F1 solution, so it is not possible to distinguish between these possibilities based on this assay. α–CTD is only 9 kDa in size, so binding to F1 DNA using fluorescence anisotropy could be difficult to detect. One way to test this possibility would be to label α–CTD with a fluorescent probe and determine whether the anisotropy changed upon addition of OmpR-P.

The secondary structure of OmpR was estimated from CD data by using the variable selection method (Compton, *et al.*, 1986; Manavalan, *et al.*, 1987) and a set of 33 proteins for comparison (provided by A. Toumadja and W. Curtis Johnson, Jr., Oregon State University). The measured contents differed from those predicted from the solved crystal structures of CheY (homologous to the N-terminal domain of OmpR, OmpRn) and OmpRc. The α-helical content of the crystal structures is 37%, whereas the average

measured α-helical content is only 27%. Though CheY and OmpRn share primary sequence homology, there may be structural differences between them which would account for these differences. Also, it cannot be assumed that the crystal structure of two separate domains of a protein is identical to the structure of the full-length protein. It is also possible that the high concentrations of protein used in crystallization have an effect on protein conformation. CD spectra of OmpR measured over a range of OmpR concentrations had different secondary structures when solved. A trend was observed in which α-helical content increased as OmpR concentration increased. It is interesting to note that the proteins in the crystal structure, which have a high α-helical content, were much more concentrated than the OmpR in the CD experiments. Thus, OmpR may change its conformation in a concentration-dependent manner. Dimerization is one possible explanation for this change in conformation. Studies using analytical ultracentrifugation are currently in progress to determine whether OmpR dimerizes in a concentration-dependent manner.

The CD spectra of OmpR showed no significant change in secondary structure upon phosphorylation or binding of F1 DNA. This does not necessarily imply that OmpR is in the same conformation in its different states. Tertiary structural changes such as movement about a hinge or local changes in the active site would not be detected by this method. OmpR-P

samples were a combination of OmpR (70%) and of OmpR-P (30%), making it difficult to detect minor changes in secondary structure. F1 DNA did not have an effect on secondary structure, suggesting that OmpR does not undergo a gross structural change upon binding to DNA.

Changes in protease cleavage patterns between different forms of a protein can reveal global structural changes that may not be detected by CD. Results from trypsin digests suggest that OmpR and OmpR-P are similar to each other but there are a few differences between them and their DNA bound forms. Bands at approximately 4 and 6 kDa were observed in the protein-DNA samples that were not seen in the apo-protein samples. Sequencing of these bands may reveal a region of the protein that is sensitive to DNA binding. I also observed that OmpR-P and OmpR:F1 DNA are more resistant to protease treatment than OmpR. Protease sensitivity often reflects the presence of solvent exposed or unstructured regions, suggesting that OmpR is more flexible than its phosphorylated or DNA bound forms.

The secondary structure content of the OmpR mutants K105R and C67S were similar to wt-OmpR. They were both able to bind DNA, but neither was phosphorylated in the presence of acetyl phosphate. It has been suggested that K105, which is located in the active site, serves as a proton donor during the phosphorylation of aspartic acid residues (Benkovic, S. J. and E. J. Sampson, 1971). In the phosphodonor EnvZ, transfer from the 3-phosphohistidine requires protonation at the N-1 atom of histidine. The conserved K105 is the

likely candidate for this function. A proton donor would also be expected to facilitate the transfer reaction from acetyl phosphate through general acid catalysis. In K105R, the arginine substitution has a different shape than the lysine and may not be an appropriate proton donor. Its bulkier side chain may change the conformation of the active site enough to prevent access of the phosphoryl group. Mutation of this conserved lysine in CheY results in a protein that dephosphorylates more slowly than the wild type (Lukat, G. *et al.*, 1991). Despite the homology among response regulators in two-component systems, there are clearly structural differences.

The rationale behind mutating the cysteine at position 67 was to remove the unique cysteine in OmpR with the intent that the purified mutant protein would be less likely to aggregate in solution. It is not yet apparent why this mutant is not phosphorylated by acetyl phosphate.

The melting temperatures of OmpR mutants K105R and C67S were the same as wt-OmpR, as determined by the intrinsic fluorescence of its tyrosines and tryptophans. The stability of the C-terminal domain was most likely measured, because it contains the unique tryptophan in OmpR as well as 3 tyrosines, whereas the N-terminal domain contains only 3 tyrosines. Thus, one cannot determine whether the stability of the N-terminal domain was affected by this method. Circular dichroism may be useful in determining the separate stabilities of both domains of OmpR. In studies on bovine rhodopsin, a cysteine to serine mutation (usually considered benign), resulted

in a protein which was unable to bind chromophore. Presumably, this was due to an increase in hydrophilicity upon substitution by serine, because an alanine mutation at the same position restored function (Davidson, F. *et al.*, 1994).

Gel shift data has shown that both half sites of the F1 binding site are required to maintain a stable OmpR-DNA complex (Huang, K. and M. Igo, 1996). This implies that dimerization of OmpR is important for stability of the interaction. It has been suggested that activation of OmpR by phosphorylation may occur via dimerization. Results from non-denaturing PAGE, gel filtration and cross-linking in the presence of dimethyl suberimidate indicate that OmpR exists as a monomer in solution (Harlocker, S. *et al.*, 1995; Jo, Y. *et al.*, 1986). A cross-linking study with OmpR in the presence of EnvZ shows formation of a 55 kDa species, likely an OmpR dimer, upon phosphorylation by EnvZ (Nakashima, K. *et al.*, 1990).

Results presented here do not clarify whether OmpR dimerizes upon phosphorylation. The molecular weight estimated from light scattering is higher for OmpR-P than for OmpR, but there are several possibilities for this increase in molecular weight. An equilibrium may exist between monomer and dimer, and phosphorylation of OmpR may shift the equilibrium to dimer formation. Another possibility is that OmpR-P has a shape which results in a higher apparent MW than that observed for OmpR. Since high concentrations of protein were used, aggregation may also have affected the

results.

Gel filtration of OmpR and OmpR-P indicated that only monomer is present in both samples. Protein concentrations were lower than those used in light scattering and the samples were further diluted as they passed over the column. If a dimer exists, it may be loosely associated and dissociate during gel filtration. Interestingly, experiments with the phosphorylated form of the closely related PhoB protein show that PhoB-P elutes from an HPLC column as a dimer at 2 mg/ml (McCleary, W., 1996). Clearly, further studies are needed to determine whether OmpR or OmpR-P dimerizes in solution.

The porin phenotypes of K105R and C67S in the *ompR*$^-$ strain MH1160 were indistinguishable from wild-type OmpR. This finding was unexpected, because neither mutant was phosphorylated *in vitro*. In this particular system, OmpR production is not regulated by the *ompB* operon as it is *in vivo*. Therefore, the porin phenotypes are most likely due to aberrantly high levels of OmpR in the cell because of expression via the plasmid. Normally, at low osmolarity, OmpF is the only porin produced, but in this system both porins were produced at low osmolarity and at high osmolarity, only OmpC was produced. This indicates that activation and repression of *ompF* is intact, but that *ompC* is improperly activated at low osmolarity. Since the dissociation constants reported in this study were approximately 200 nM for unphosphorylated OmpR, this result is not surprising.

Our results are consistent with previous studies that reported when OmpR was over-expressed in a strain containing a non-phosphorylatable EnvZ mutant, *ompC* expression was increased at low osmolarity and *ompF* expression was lower than in a wt strain (Forst, S. *et al.*, 1988). At high osmolarity, *ompF* was repressed and *ompC* was activated, as is evident in Figure 12. This is not unexpected in light of my results which indicate that unphosphorylated OmpR has a significantly higher affinity for C1 compared to F1 (Table 2).

Conclusions

1. The mechanism by which OmpR activates and represses transcription of the porin genes is not fully understood. Findings presented here demonstrate that phosphorylation enhances binding of OmpR to its promoter regions by at least ten-fold.

2. The presence of the F1 binding site confers high affinity to the *ompF* promoter. The C1 site has an even greater affinity for OmpR-P than F1. This result indicates that porin regulation cannot be accounted for by the simple affinity model alone.

3. Phosphorylation or DNA binding do not drastically alter the secondary structure or protease cleavage pattern of OmpR.

4. The OmpR mutants K105R and C67S are similar to wt-OmpR in their secondary structure, but both mutations affect the N-terminal phosphorylation domain, as evidenced by their inability to be phosphorylated

in vitro.

Aiba, H., N. Kato, M. Tsuzuki and T. Mizuno (1994) Mechanism of gene activation by the *Escherichia coli* positive regulator, OmpR: a mutant defective in transcripitional activation. *FEBS Letters* **351:** 303-307.

Baikolov, I., I. Schroder, M. Kaczor, Kazimierz Grzeskowiak, R. P. Gunsalus and R. E. Dickerson (1996). Structure of the *Escherichia coli* Response Regulator NarL. *Biochemistry* **35:** 11053-11061.

Benkovic, S. J. and E. J. Sampson (1971) Structure-reactivity correlation for the hydrolysis of phosphoramidite monoions *Journal of the American Chemical Society***93:** 4009-4016.

Compton, L. A., Matthews, C. K. and Johnson, W. C., Jr. (1987) The conformation of T4 bacteriophage dihydrofolate reductase from circular dichroism *Journal of Biological Chemistry* **262:** 13039-13043.

Compton, L. A., and W. C. Johnson Jr. (1986). Analysis of protein circular dichroism spectra for secondary structure using a simple matrix multiplication. *Analytical Biochemistry.* **155:** 155-167.

Davies, J. K. and P. Reeves, (1975) Genetics of resistance of colicins in *Escherichia coli* K12: cross-resistance among colicins of group A *Journal of Bacteriology*. **123:** 102-117.

Datta, D. B., B. Arden and U. Henning (1976) Major proteins of the *Escherichia coli* outer cell envelope membrane as bacteriophage receptors *Journal of Bacteriology*. **131:** 821-829.

Davidson, F., Loewen, P. C. and A. G. Khorana (1994) Structure and Function in rhodopsin: replacement by alanine of cysteine residues 110 and 187, components of a conserved disulfide bond in rhodopsin, affects the light activated metarhodopsin II state *Proceedings of the National Academy of Sciences* **91:** 4029-4033.

Delgado, J., and M. Inouye (1993) Identification of a phosphorylation site and functional analysis of conserved aspartic acid residues of OmpR, a transcriptional activator for*ompF* and *ompC* in *Escherichia coli. Molecular Microbiology* **10:** 1037-1047.

Ernsting, B. R., M. R. Atkinson, A. J. Ninfa, and R. G. Matthews (1992). Characterization of the regulon by the leucine-responsive regulatory protein in *Escherichia coli Journal of Bacteriology* **174:** 1109-1118.

Forst, S., J. Delgado and M. Inouye (1989) Phosphorylation of OmpR by the

osmosensor EnvZ modulates expression of the *ompF* and *ompC* genes in *Escherichia coli. Proceedings of the National Academy of Science USA* **86:** 6052-6056.

Forst, S., J. Delgado, J. Ramakrishnan and M. Inouye (1988) Regulation of *ompC* and *ompF* expression in the absence of *envZ Journal of Bacteriology* **170:** 5080-5085.

Forst, S., D. Comeau, S. Norioka and M. Inouye (1987) Localization and membrane topology of EnvZ, a protein involved in osmoregulation of OmpF and OmpC in *Escherichia coli. Journal of Biological Chemistry USA* **262:** 16433-16438.

Graeme, C. K., G. May, E. Bremer and C. F. Higgins (1989) Osmotic regulation of porin expression: a role for DNA supercoiling *Molecular Microbiology* **3:** 1287-1294.

Harlocker, S. L. (1996) Characterization of the binding of OmpR, a transcription factor in *Escherichia coli,* to the upstream regulatory sequences of *ompF.* [PhD Thesis]. Rutgers University, New Brunswick, NJ.

Harlocker, S. L., L. Bergstrom and M. Inouye (1995) Tandem binding of six OmpR proteins to the *ompF* upstream regulatory sequence of *Escherichia coli. Journal of Biological Chemistry USA* **270:** 26849-26856.

Hess, J. F., R. Bourret and M. I. Simon (1988) Histidine phosphorylation and phosphoryl group transfer in bacterial chemotaxis *Nature* **336:** 139-143.

Hoch, J. A. and T. J. Silhavy (1995) Porin Regulon of *Escherichia coli.* In *Two Component Signal Transduction.* (Hoch, J. A. and Silhavy, T. J., eds.). American Society for Microbiology, Washington, DC.

Huang, K. and M. Igo (1996) Identification of the bases on the *ompF* regulatory region which interact with the transcription factor OmpR *Journal of Molecular Biology* **262:** 615-628.

Huang, K. and M. Igo (1994)A distant upstream site involved in the negative regulation of the *Escherichia coli ompF* gene *Journal of Bacteriology* **176:** 1309-1315.

Igarashi, K., and A. Ishihama (1991) Bipartite functional map of the *E. coli,* RNA polymerase alpha subunit: involvement of the C-terminal region in transcription activation by c-AMP-CRP. *Cell* **65:** 1015-1022.

Igo, M., J. M. Slauch and T. J. Silhavy (1990) Signal transduction in bacteria: kinases that control gene expression. *New Biologist* **2:** 5-9.

Igo, M., A. J. Ninfa, and T. J. Silhavy. (1989a) A bacterial environmental sensor that functions as a protein kinase and stimulates transcriptional activation. *Genes and Development* **3:** 598-605.

Igo, M., A. J. Ninfa, J. B. Stock, and T. J. Silhavy. (1989b) Phosphorylation and dephosphoylation of a bacterial transcriptional activator by a transmembrane receptor. *Genes and Development* **3:** 1725-1734.

Igo, M. and T. J. Silhavy (1988) EnvZ, a trans-membrane environmental sensor of *Escherichia coli* K12 is phosphorylated *in vitro. Journal of Bacteriology* **170:** 5971-5973.

Jo, Y., F. Nara, S. Ichihara, T. Mizuno and S. Mizushima (1986) Purification and characterization of the OmpR protein, a positive regulator involved in osmoregulatory expression of the *ompF* and *ompC* genes in *Escherichia coli. Journal of Biological Chemistry USA* **261:** 15252-15256.

Kenney, L. J., M. Bauer and T. J. Silhavy (1995) Phosphorylation-dependent conformational changes in OmpR, an osmoregulatory DNA-binding protein of *Escherichia coli. Proceedings of the National Academy of Science USA* **92:** 8866-8870.

Liljestrom, P. (1986) the EnvZ protein of *Salmonella typhimurium* LT-2 and *Escherichia coli* K12 is located in the cytoplasmic membrane. *FEMS Microbiological Letters* **36:** 145-150.

Liljestrom, P. (1986) Structure and expression of the *ompB* operon of *Salmonella typhimurium* and *Escherichia coli,* Thesis Dissertation. University of Helsinki, Helsinki, Finland.

Lukat, G. S., W. McCleary, A. M. Stock, and J. B. Stock (1992) Phosphorylation of bacterial response regulator proteins by low molecular weight phospho-donors. *Proceedings of the National Academy of Science USA* **89:** 718-722.

Lukat, G. S., B. H. Lee, J. M. Mottonen, A. M. Stock and J. B. Stock (1991) Roles of the highly conserved aspartate and lysine residues in the response regulator of bacterial chemotaxis. *Journal of Biological Chemistry* **266:** 8348-8354.

Lukat, G. S., A. M. Stock, and J. B. Stock (1990) Divalent metal ion binding to the CheY protein and its significance to phosphotransfer in bacterial

chemotaxis *Biochemistry* **28:** 5436-5442.

Maeda, S., K. Takayanagi, Y. Nishimura, T. Maruyama, K. Sato, and T. Mizuno (1991) Activation of the osmoregulated *ompC* gene by the OmpR protein in *Escherichia coli.* A study involving synthetic OmpR binding sequences *Journal of Biochemistry (Tokyo)* **110(3):** 324-327.

Maeda, S., and T. Mizuno (1990) Evidence for multiple OmpR-binding sites in the upstream activation sequence of the *ompC* promoter in *Escherichia coli:* a single OmpR binding site is capable of activating the promoter *Journal of Bacteriology* **172:** 501-503.

Makino, K., H. Shinagawa, M. Amemura and A. Nakata (1986) Nucleotide sequence of the *phoB* gene, the positive regulatory gene for the phosphate regulon of *Escherichia coli Journal of Molecular Biology* **190:** 37-44.

Manavalan, Parthasarathy and W. Curtis Johnson Jr. (1987) Variable selection method improves the prediction of protein secondary structure from circular dichroism. *Analytical Biochemistry.* **167:** 76-85.

Martinez-Hackert, E. and A. M. Stock (1997) The DNA-binding domain of OmpR: crystal structures of a winged helix-turn-helix transcription factor *Structure* **5:** 109-124.

McCleary, W., (1996) The activation of PhoB by acetylphosphate *Molecular Microbiology* **20:** 1155-1163.

McCleary, W., J. B. Stock and A. J. Ninfa (1993) Is acetyl phosphate a global signal in *Escherichia coli? Journal of Bacteriology* **175:** 2793-2798.

Mizuno, T. (1987a) Static bend of DNA helix at the activator recognition site of the *ompF* promoter in *Escherichia coli. Gene* **54:** 57-64.

Mizuno, T., and S. Mizushima (1987b) Isolation and characterization of deletion mutants of *ompR and envZ,* regulatory genes for expression of the outer membrane proteins OmpC and OmpF in *Escherichia coli. Journal of Biological Chemistry* **257:** 13692-13698.

Mizuno, T., E. T. Wurtzel and M. Inouye (1982) Osmoregulation of gene expression III. DNA sequence of the *envZ* gene of the *ompB* operon of *Escherichia coli* and characterization of its gene product. *Journal of Bacteriology* **175:** 2793-2798.

Nakashima, K., K. Kanamuru, H. Aiba and T. Mizuno (1991) Signal

transduction and osmoregulation in *Escherichia coli. Journal of Biological Chemistry* **266:** 10775-10780.

Nikaido, H., and M. Vaara (1985) Molecular basis of bacterial outer membrane permeability. *Microbiol. Rev.* **49:** 1-32.

Nikaido, H., and M. Vaara (1987) Outer membrane, p 7-22. *In* F. C. Neidhardt, J. L. Ingraham, K. Low, B. Magasanik, M. Schaechter and H. E. Umbarger (ed.), *Escherichia coli* and *Salmonella typhimurium:* cellular and molecular biology. American Society for Microbiology, Washington, D. C.

Nixon, B. T., C. Ronson, and F. Ausabel (1986) Two component regulatory system responses to environmental stimuli share strongly conserved domains within the nitrogen assimilation regulatory genes *ntrB* and *ntrC* *Proceedings of the National Academy of Science USA* **83:** 7850-7854.

Payne, J. W., and C. Gilvarg (1968) Size restriction on peptide utilization in *Escherichia coli. Journal of Biological Chemistry* **243:** 6291-6299.

Pratt, L. A. and T. J. Silhavy (1994) OmpR mutants specifically defective for transriptional activation *Journal of Molecular Biology* **243:** 579-594.

Pratt, L. A. and T. J. Silhavy (1995) Porin Regulon of *Escherichia coli.* In *Two Component Signal Transduction.* (Hoch, J. A. and Silhavy, T. J., eds.), pp. 105-127. American Society for Microbiology, Washington, DC.

Ramani, N., L. Huang and M. Freundlich (1992) *In vitro* interactions of intergration host factor with the *ompF* promoter-regulatory region of *Escherichia coli Molecular Genes and Genetics* **231:** 248-255.

Rampersaud, A., S. Harlocker and M. Inouye (1994) The OmpR protein of *Escherichia coli* binds to sites in a hierarchical manner determined by its degree of phosphorylation *Journal of Biological Chemistry* **269:** 12559-12566.

Roberts, D.L., D. W. Bennet, and S. A. Forst (1994) Identification of the site of phosphorylation on the osmosensor, EnvZ, of *Escherichia coli. Journal of Biological Chemistry* **269:** 8728-8733.

Russo, F., J. M. Slauch and T.J. Silhavy (1993) Mutations that affect separate functions of OmpR, the phosphorylated regulator of porin transcription in *Escherichia coli. Journal of Molecular Biology* **231:** 261-273.

Russo, F. and T.J. Silhavy (1991) EnvZ controls the concentration of phosphorylated OmpR to mediate osmoregulation of the porin genes. *Journal*

of Molecular Biology **222:** 567-580.

Sarma, V. and P. Reeves (1977) Genetic locus (*ompB)* affecting a major outer-membrane protein in *Escherichia coli* K12. *Journal of Bacteriology* **132:** 23-27.

Schagger, H., and G. vonJagow (1987) Tricine-sodium dodecyl sulfate-polyacrylamide gel electrophoresis for the separation of proteins in the range from 1 to 100 kDa *Analytical Biochemistry* **166:** 368-379.

Scott, N. W. and C. R. Harwood (1980). Studies on the influence of the cyclic AMP system on major outer membrane proteins of *Escherichia coli* K12. *FEMS Microbiological Letters* **9:** 95-98.

Sharif, T. R. and M. Igo (1993) Mutations in the alpha subunit of RNA polymerase that affect the regulation of porin gene transcription in *Escherichia coli* K12 *Journal of Bacteriology* **175:** 5460-5468.

Slauch, J. M., F. Russo and T. J. Silhavy (1991) Suppressor mutations in *rpoA* suggest that OmpR controls transcription by direct interaction with the alpha subunit of RNA polymerase *Journal of Bacteriology* **173:** 7501-7510.

Stock, J. B., A. Ninfa and A. M. Stock (1989) Protein phosphorylation and regulation of adaptive responses in bacteria *Microbiological Reviews* **53:** 450-490.

Stock, A. M., J. Mottonen, J. B. Stock, and C. E. Schutt (1989) The three-dimensional structure of CheY, the response regulator of bacterial chemotaxis *Nature.* **337:** 745-749.

Suzuki, M and S. E. Brenner (1995) Classification of multi-helical DNA binding domains and application to predict the DBD structures of sigma factor, LysR, OmpR/PhoB, CENP-B, Rapl, and XylS/Ada/AraC *FEBS Letters* **372:** 215-221.

Tokishita, S., A. Kojima and T. Mizuno (1991) Transmembrane signal transduction and osmoregulation in *Escherichia coli Journal of Biological Chemistry* **266:** 6780-6785.

Tsui, P., V. Helu and M. Freundlich (1988) Altered osmoregulation of *ompF* in integration host factor mutants of *Escherichia coli* . *Journal of Bacteriology* **170:** 4950-4953.

Tsuzuki, M., H. Aiba, and T. Mizuno (1994) Gene activation by the *Escherichia coli* positive regulator, OmpR: phosphorylation-independeent mechanism of

activation by an OmpR mutant. *Journal of Molecular Biology* **242:** 607-613.

VanAlphen, W. and B. Lugtenberg (1977) Influence of osmolarity of the growth medium on the outer membrane protein pattern of *Escherichia coli*. *Journal of Bacteriology* **131:** 623-630.

Volz, K., and P. Matsumura (1991) Crystal structure of *Escherichia coli* CheY refined at 1.7 A resolution *Journal of Biological Chemistry* **266:** 15511.

Volz, K. (1993) Structural conservation in the CheY superfamily *Biochemistry* **32:** 11741-11752.

Wanner, B. L. and M. R. Wilmes-Riesenberg (1992) Involvement of phosphotransacetylase, acetate kinase, and acetyl phosphate synthesis in the control of the phosphate regulon in *Escherichia coli*. *Journal of Bacteriology* **174:** 2124-2130.

Wurtzel, E.T., M. Y. Chou and M. Inouye (1982) Osmoregulation of gene expression I. DNA sequence of the *ompR* gene of the *ompB* operon of *Escherichia coli* and characterization of its gene product *Journal of Biological Chemistry* **257:** 13685-13691.

Yang, Y. and M. Inouye (1991) Intermolecular complementation between two defective mutant signal-transduction receptors of *Escherichia coli*. *Proceedings of the National Academy of Sciences USA.* **88:** 11057-11061.